CrossMark

Recent state of nanofluid in automobile cooling systems

Hong Wei Xian[1] · Nor Azwadi Che Sidik[1] · G. Najafi[2]

Abstract

Nanofluid that made up of fluid and solid nanoparticles has gained attention from diverse fields due to its superior thermophysical properties to enhance the performance of different systems which require flowing medium with excellent heat transfer behavior. Many past researchers have proven that conventional heat transfer fluid can be replaced by the rising nanotechnology–nanofluid which showed astonishing performance under different circumstances. In this paper, we attempt to present a recent review on the consequences of implantation of nanofluid, especially in vehicle engine cooling system and other heat transfer applications such as solar collector, electronics cooling system, flow boiling and thermal energy storage system. Thermophysical properties and heat transfer performance of nanofluids obtained in simulation, test rigs and even real vehicle engine experiments are discussed thoroughly. Models and correlations used by past researchers to compute thermophysical properties are also included. In the last part, various advantages from using nanofluid are summarized, and suggestions for research gap between past studies are discussed to further improve the investigation work in the future.

Abbreviations

ANN	Artificial neural network
ASHRAE	American Society of Heating, Refrigerating and Air-Conditioning Engineers
DWCNT	Double-walled carbon nanotube
EG	Ethylene glycol
ENF	Magnetic electrolyte nanofluid
FMWCNT	Functionalized multi-walled carbon nanotube
F-SWCNT	Functionalized single-walled carbon nanotube
MWCNT	Multi-walled carbon nanotube
ppm	Parts per million (mg L^{-1})
RBF	Radial basis function
Rpm	Revolution per minute

List of symbols

c_p	Specific heat capacity at constant pressure (J kg^{-1} K^{-1})
d	Mean diameter (nm)
k	Thermal conductivity (W m^{-1} K^{-1})
n	Shape factor
Nu	Nusselt number
Pe	Peclet number
Pr	Prandtl number
Re	Reynolds number
T	Temperature (vary with correlations proposed by past researchers in K or °C)

Greek symbols

α	Thermal diffusivity (m^2 s^{-1})
β	Volumetric coefficient of thermal expansion (1/K)
η	Ratio of nanolayer thickness to original particle radius (for reference numbered 39)
μ	Dynamic viscosity (kg m^{-1} s^{-1})
ρ	Density (kg m^{-3})
φ	Volume concentration (%)

Subscripts and superscripts

B	Boltzmann constant (for reference numbered 44)
eff	Effective

✉ Nor Azwadi Che Sidik
  azwadi@utm.my

1 Malaysia – Japan International Institute of Technology (MJIIT), University Teknologi Malaysia Kuala Lumpur, Jalan Sultan Yahya Petra (Jalan Semarak), 54100 Kuala Lumpur, Malaysia

2 Tarbiat Modares University, Tehran, Iran

f	Base fluid
fr	Freezing point of base fluid
hnf	Hybrid nanofluid
max	Maximum
nf	Nanofluid
np	Solid nanoparticles

Introduction

With expeditious development of science and technology, nanotechnology is utilized in diverse applications, especially heat exchanger, electronics cooling, solar energy, biomedical, refrigeration and thermal energy storage system. The miniaturization of devices and materials is prevailing trend nowadays. One of the most common nanoscience applications today is called nanofluid. Nanofluid was first proposed by Choi [1], and it is basically a two-phase system, which consists of base fluid and suspended solid nanoparticles. Nanoparticles typically sized less than 100 nm and usually made up of materials listed in Fig. 1.

As nanoparticles are dispersed into base fluid, rheological behavior and thermophysical properties of base fluid will be greatly influenced. Among all thermophysical properties, thermal conductivity plays a vital role in most engineering applications as it represents the capability of a material to transfer heat. Figure 2 shows the difference of thermal conductivity among commonly used components in nanofluids [2]. It can be seen that thermal conductivity of fluid is significantly lower when compared to that of solid particles. Thus, many past researchers studied on the effects of mixing solid nanoparticles into fluids and observed that nanofluids show superb heat transfer characteristics [3–5] and heat transfer performance [6–10] compared to base fluid.
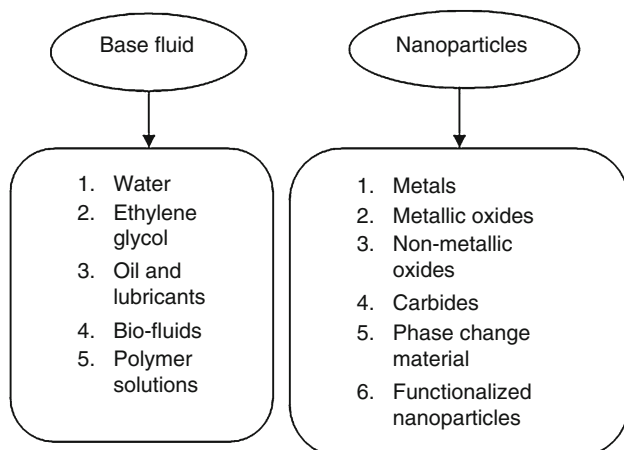

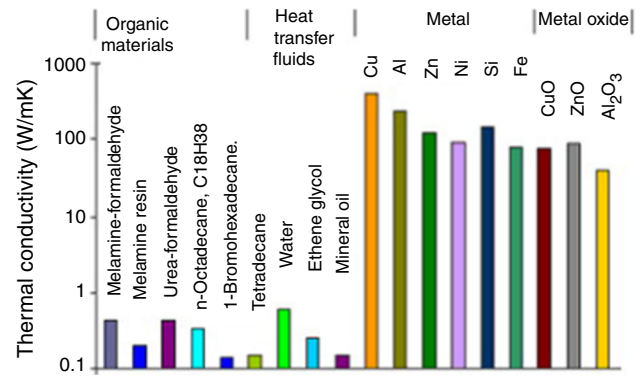Fig. 1 Common material for base fluid and nanoparticles

Fig. 2 Thermal conductivities of different polymers, liquids and solids [2] (License Number: 4344040672984)

Up to now, there is only a comprehensive review focused on automobile engine cooling system with utilization of nanofluid as nanocoolant [11]. To the best of authors' knowledge, there are some past researches about applications of nanofluid in real vehicle engine and automobile radiators. It is found that there is still no review reported on behavior of nanofluids in different types of automobile radiators. Hence, authors are inspired to include this discrepancy and provide an extensive review on nanofluids in automobile radiator cooling system and other major applications which involve impregnation of nanofluid to improve thermophysical properties, efficiency and heat transfer performance.

Thermophysical properties of nanofluid

Due to exceptional thermal properties of solid material compared to fluid, Stephen Choi [1] expected nanofluid could be possible substitute for conventional heat transfer fluid. Since then, nanofluid started to draw attention of researchers from different fields and they looked up the outcome from using nanofluid. One of the earliest efforts in measuring thermal conductivity was carried out by Lee et al. [12]. Transient hot-wire method was used for measuring purpose, and it was found that low concentration of oxide nanofluid showed surprisingly high thermal conductivity than base fluid. Since then, many researchers conducted studies on thermophysical properties of nanofluid in different environments.

Experimental studies

In 2010, Kole and Dey [13] measured viscosity of water/propylene glycol mixed with alumina nanoparticles using Brookfield programmable viscometer. Their results showed that relationship between viscosity and temperature of the nanocoolant agreed well with empirical correlation

proposed by Namburu et al. [14] in year 2007, with maximum deviation of less than 2%. In Fig. 3, dots indicate their obtained results, while dotted lines are Namburu's correlation.

A major study by Wang et al. [15] included the dispersion of two different nanoparticles (Al_2O_3 and CuO) into water, engine oil, ethylene glycol and vacuum pump fluid. Steady-state parallel-state method was used to measure thermal conductivity, and they reported that thermal conductivities of all nanofluids were higher than respective base fluids. Another novel study on investigating the relationship between temperature and thermal conductivity was carried out by Das and his team [16]. From their result, it was observed that the enhancement of thermal conductivity for 4 vol% Al_2O_3–water nanofluid was increased from 9.4 to 24.3% when temperature increased from 21 to 51 °C.

Chen and Jia [17] reported the enhancement of thermal conductivity of 3% when mass fraction of TiO_2 in water/ethylene glycol was varied from 0.5 to 5%. Measurement of thermophysical properties of 13 nm Al_2O_3–water/ethylene glycol as car radiator coolant was taken by Elias and his squad [18] in 2014. Their result revealed that maximum enhancement for thermal conductivity, viscosity and density was 8.30, 150 and 2.91%, respectively, at 1 vol% Al_2O_3 in the range of 10–15 °C.

Kh and his team [19] investigated thermophysical and rheological properties of water/ethylene glycol nanofluid with functionalized graphene nanoplatelets. Their results showed that the thermal conductivity of 0.2 mass% nanoplatelets was about 58% higher than that of base fluid at 65 °C; meanwhile, dynamic viscosity showed 4.86% of increment at the same conditions. Selvam and his group [20] reported that thermal conductivity of 0.45 vol%

graphene in water/ethylene glycol nanofluid increased thermal conductivity by 18% but decreased specific heat capacity by 8%.

Multi-walled carbon nanotube (MWCNT) nanofluid in a square enclosure was studied by Garbadeen et al. [21]. They measured thermal conductivity and viscosity using KD2 Pro and SV10 Sine-wave Vibro Viscometer, respectively. For 0–1 vol% of MWCNT, maximum enhancement of thermal conductivity and viscosity is found to be 6 and 58%, respectively, when compared to water. Thakur et al. [22] also measured thermophysical properties of same nanofluid at temperature of 30–70 °C and concentration of 0–0.8 vol%. They reported that 23% of enhancement in thermal conductivity was found at 0.8 vol% and 70 °C. Moreover, specific heat was found to decrease when nanoparticle concentration was increased which in conformity with experimental work by Ilyas et al. [23] who worked on MWCNT–thermal oil.

Modification of surface properties of SiO_2 nanoparticles by depositing copper was carried out by Amiri et al. [24]. For 50–80 nm modified SiO_2 nanoparticles produced, they used transient hot-wire method to obtain thermal conductivity of the nanoparticles dispersed in water. From their experiment, thermal conductivity could be enhanced up to 11% by using less than 1 vol% modified nanoparticles. In addition to that, they claimed that this new nanocomposite has better resistance against oxidation in air compared to pure metal.

Few researchers investigated the relationship between base fluid ratio and thermophysical properties. Abdolbaqi and his team [25] prepared water-/bioglycol-based SiO_2 nanofluid in 20:80 and 30:70% base fluid ratio. Temperature and nanoparticle concentration were varied between 30–80 °C and 0.5–2.0 vol% in the experiment. For 20:80%

Fig. 3 Relationship between log viscosity and temperature [13]
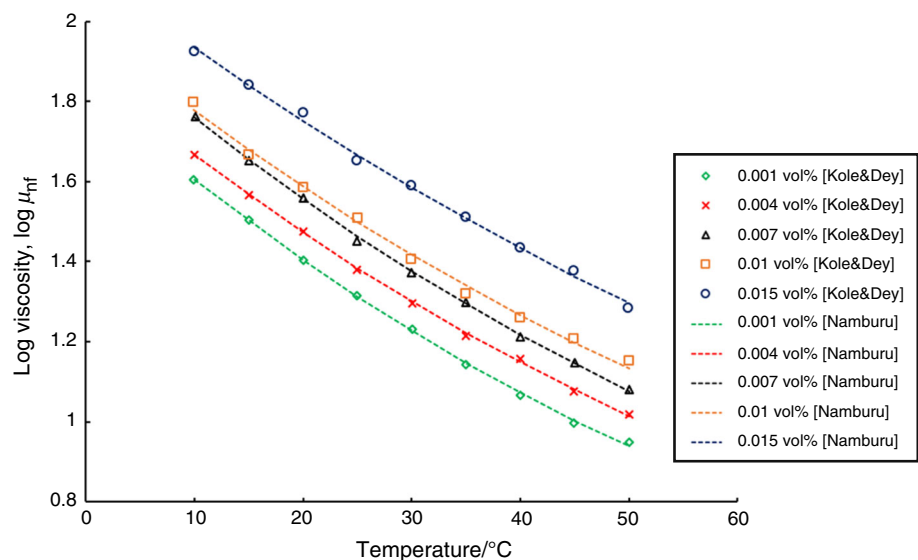
base fluid nanofluid, 7.2% of thermal conductivity enhancement was obtained at 2.0 vol% SiO_2 and 70 °C. Besides that, viscosity was increased up to 29.8 and 53.4% at 30 °C and 60 °C, respectively, for 30:70% base fluid nanofluid with 2.0 vol% SiO_2. With the same intention, Chiam et al. [26] prepared Al_2O_3 nanofluids with different base fluid ratios (40:60, 50:50 and 60:40) and tested them from 30 to 70 °C. They highlighted that higher portion of ethylene glycol in mixture led to increment of thermal conductivity and decrement of viscosity. Their results revealed 12.8% of thermal conductivity enhancement for 40:60 base fluid and 50% increment of dynamic viscosity for 60:40 base fluid, with 1.0 vol% Al_2O_3.

Glycerin (G13) was mixed by Sundari and his group [27] with 0.05–0.15 vol% of Al_2O_3 to measure the thermophysical properties from 30 °C to 50 °C. They varied the operating temperature from 30 °C to 50 °C, and the viscosity was decreased by 33.84%. At 40 °C, 0.15 vol% Al_2O_3 increased thermal conductivity for 46.15%. Furthermore, it was found that surface tension and pH value were inversely proportional to temperature.

Nabil et al. [28] prepared and measured a hybrid nanofluid that made up of TiO_2–SiO_2 (50:50) and water/ethylene glycol (60:40). Maximum error of 1.6% was found when the measured data were compared to ASHRAE. For 3.0 vol% nanoparticles, maximum thermal conductivity was enhanced by 22.8% and average relative viscosity obtained 62.5% increment. They suggested that this hybrid nanofluid could benefit heat transfer applications with the addition of at least 1.5% vol% nanoparticles concentration.

Functionalized single-walled carbon nanotube (F-SWCNT) was dispersed in water/ethylene glycol by Adhami et al. [29] for determining the thermophysical properties. From 0.025 to 0.65% volume fraction, temperature showed huge impact on thermal conductivity when volume fraction is more than 0.53%. Additionally, they compared alumina–water/ethylene glycol nanofluid with existing nanofluid and found that only 5% of increment in thermal conductivity from alumina nanofluid, whereas F-SWCNT nanofluid showed 52.7% under identical conditions.

Iqbal and his team [30] presented thermal conductivities of different deionized water-based nanofluids at same volume concentration. At 1 vol% nanoparticles, respective thermal conductivity increment for Al_2O_3, SiO_2 and ZrO_2 was 10.13, 6.5 and 8.5%. As other researchers, this team also mentioned that viscosity is directly proportional to nanoparticles concentration.

For hybrid Fe_2O_3/MWCNT water-based nanofluid, Chen et al. [32] varied the concentration of Fe_2O_3 nanoparticles and measured the thermal conductivity. With 0.02 mass% Fe_2O_3 and 0.05 mass% MWCNT, they obtained 27.7% of enhancement in thermal conductivity which was higher than 0.02 mass% MWCNT and 0.02 mass% Fe_2O_3 nanofluid alone. However, when they added more Fe_2O_3 (> 0.02 mass%) in the hybrid suspension, thermal conductivity decrement was observed. They proposed that high concentration of nanoparticles would lead to agglomeration easily, in which affecting heat transfer performance significantly.

Summary of experimental studies on thermophysical properties of nanofluids reviewed earlier is tabulated in Table 1, with some other undiscussed researches.

Empirical correlations and equations

Based on the literature review, different models were used by former researchers to compute thermophysical properties. Maxwell model [42] is one of the earliest models to compute thermal conductivity of solid–liquid mixture and commonly modified by former researchers to develop new thermal conductivity models. Hamilton and Crosser [43] modified Maxwell model and proposed shape factor (n) which can be used for other nanoparticles shapes rather than spherical. Yu and Choi [44] expanded Maxwell model by assuming a solid-like nanolayer with thickness (h) surrounded a spherical nanoparticle with radius (r) and thus form a bigger radius of $r + h$ nanoparticle. Koo and Kleinstreuer [45] added the effects of mixture temperature, nanoparticle size and concentration, Brownian motion of nanoparticles into Maxwell model. Pak and Cho [46] suggested that thermal conductivity is mainly affected by dispersion of nanoparticles. On the other side, Maiga et al. [47] suggested that some past researchers underestimated viscosity and thermal conductivity of nanofluids, and thus, they proposed few correlations using least-square curve fitting of past experimental data. Similarly, Corcione [48] extracted experimental data from past studies and proposed effective thermal conductivity and viscosity correlations with about 1.85% of standard deviation error.

For dynamic viscosity models, Einstein model [49] is the earliest model developed. It was then modified by Brinkman to add in viscosity and volume fraction of both nanoparticles and base fluid. Nanoparticles concentration was taken into account by Wang et al. [15] when calculating viscosity of nanofluid. Batchelor [50] considered the effect of Brownian motion in a suspension containing rigid spherical nanoparticles. On the other hand, Gherasim et al. [51] considered only spherical nanoparticles in their proposed model. Brownian motion of nanoparticles was considered as one of the factors affecting effective viscosity, as proposed by Tiwari and Das [52].

Khanafer and Vafai [53] tested the reliability of the first density equation in Table 1. Also, they developed a correlation for density of aluminum oxide based on experimental data from Ho et al. [54]. For specific heat capacity

Table 1 Summary of experimental studies of thermophysical properties for nanofluids

Authors	Thermophysical properties	Nanoparticles	Base fluid	Findings
Lee et al. [12]	Thermal conductivity	Al_2O_3 and CuO	No info	Low concentration of nanoparticles performed better than base fluid
Kole and Dey [13]	Viscosity	Al_2O_3	Water/proplyene glycol	Viscosity depends mainly on temperature
Wang et al. [15]	Thermal conductivity	Al_2O_3 and CuO	Water	Thermal conductivities of all nanofluids were higher than respective base fluids
			Engine oil	
			Ethylene glycol Vacuum pump fluid	
Das and his team [16]	Thermal conductivity	Al_2O_3	Water	4 vol% Al_2O_3 increased thermal conductivity up to 24.3% at 51 °C
Chen and Jia [17]	Thermal conductivity	TiO_2	Water/ethylene glycol	Thermal conductivity enhancement of 3% with 0–0.5% TiO_2
Elias and his squad [18]	Thermal conductivity, viscosity and density	Al_2O_3	Water/ethylene glycol	1 vol% Al_2O_3 increased thermal conductivity, viscosity and density by 8.30, 150 and 2.91%, respectively
Kh and his team [19]	Thermal conductivity and viscosity	Functionalized graphene	Water/ethylene glycol	0.2 mass% nanoplatelets increased thermal conductivity and viscosity for about 58 and 4.86% at 65 °C
Selvam and his squad [20]	Thermal conductivity and specific heat capacity	Graphene	Water/ethylene glycol	0.45 vol% graphene increased thermal conductivity by 18% but decreased specific heat capacity by 8%
Garbadeen et al. [21]	Thermal conductivity and viscosity	MWCNT	Water	0–1 vol% of MWCNT increased thermal conductivity and viscosity by 6 and 58%
Thakur et al. [22]	Thermal conductivity	MWCNT	Water	0.8 vol% of MWCNT increased thermal conductivity by 23% at 70 °C
Amiri et al. [24]	Thermal conductivity	SiO_2 (modified surface properties)	Water	Thermal conductivity increased by 11% by less than 1 vol% nanoparticles
Abdolbaqi and his team [25]	Thermal conductivity and viscosity	SiO_2	Water/bioglycol	At 2.0 vol% SiO_2, 7.2% thermal conductivity enhancement was obtained at 70 °C—(20:80) base fluid
				Viscosity was increased by 29.8 and 53.4% at 30 °C and 60 °C, respectively—(30:70) base fluid
Chiam et al. [26]	Thermal conductivity	Al_2O_3	Water/ethylene glycol	12.8% increment in thermal conductivity—(40:60) base fluid
	Viscosity			50% increment in viscosity–(60:40) base fluid
Sundari and his group [27]	Thermal conductivity	Al_2O_3	Glycerin (G13)	0.15 vol% Al_2O_3 increased thermal conductivity for 46.15% at 40 °C
Nabil and his lineup [28]	Thermal conductivity and viscosity	TiO_2–SiO_2 (50:50)	Water/ethylene glycol (60:40)	3.0 vol% nanoparticles enhanced thermal conductivity by 22.8% and average relative viscosity by 62.5%
Adhami et al. [29]	Thermal conductivity	F-SWCNT	Water/ethylene glycol	From 0.025 to 0.65% volume fraction, temperature showed huge impact on thermal conductivity when volume fraction is more than 0.53%
				F-SWCNT nanofluid showed more increment than Al_2O_3 nanofluid
Iqbal and his team [30]	Thermal conductivity	Al_2O_3, SiO_2 and ZrO_2	Deionized water	At 1 vol% nanoparticles, respective thermal conductivity enhancement for Al_2O_3, SiO_2 and ZrO2 was 10.13, 6.5 and 8.5%
Chen et al. [32]	Thermal conductivity	Fe_2O_3 + MWCNT	Water	With 0.02 mass% Fe_2O_3 and 0.05 mass% MWCNT, they obtained 27.7% of enhancement in thermal conductivity
Murshed et al. [32]	Thermal conductivity	TiO_2	Deionized water	5 vol% TiO_2 enhanced thermal conductivity of base fluid by 30%
Assael et al. [33]	Thermal conductivity	MWCNT	Water	0.6 vol% MWCNT showed 38% of maximum enhancement compared to water
Xuan and Li [34]	Thermal conductivity	CuO	Water	2.5 and 7.5 vol% CuO generated enhancement of 24 and 78%, respectively
Hong et al. [35]	Thermal conductivity	Fe	Ethylene glycol	0.55 vol% Fe showed 18% of enhancement

Table 1 (continued)

Authors	Thermophysical properties	Nanoparticles	Base fluid	Findings
Chen et al. [36]	Thermal conductivity	TiO$_2$	Water	2.5 mass% TiO$_2$ showed 3 and 5% increment of thermal conductivity at 25 and 40 °C, respectively
Chougule and Sahu [37]	Thermal conductivity	Al$_2$O$_3$ CNT	Water	At 80 °C, CNT nanofluid showed extra 58% of enhancement compared to Al$_2$O$_3$ nanofluid at 1.0 vol%
Li et al. [38].	Thermal conductivity	SiC	Water/ethylene glycol	At 50 °C, 0.5 vol% of SiC nanoparticles could enhance thermal conductivity up to 53.81%
Esfe and Saedodin [39]	Thermal conductivity	MgO	Water	Heat transfer was increased when diameter of nanoparticles decreased, Reynolds number and nanoparticles concentration were increased
Afshari et al. [40]	Viscosity	MWCNT–Al$_2$O$_3$	Water–EG (80:20%)	Dynamic viscosity increased with increasing concentration and decreasing temperature. At 0.75 and 1% vol%, the nanofluid showed pseudoplastic non-Newtonian behavior
Ahammed et al. [41]	Viscosity	Graphene	Water	When concentration of graphene was kept at 0.15 vol%, viscosity of water showed average increment of 47.12% and decrement of 18.7% was observed for surface tension at 50 °C

models, the authors [53] compared the first and second models in Table 1 with experimental data from past researchers. It was found that second model could give more accurate results due to an assumption in the equation which considers thermal equilibrium between base fluid and nanoparticles.

Although there are many available equations and correlations in the literature, different assumptions were made, and this led to distinct results among past researchers even though similar approaches were used on same nanoparticles, as reported in the past study [53]. Hence, general correlations for thermal conductivity and viscosity of Al$_2$O$_3$–water were developed by combining past experimental data:

$$\frac{k_{\text{eff}}}{k_{\text{f}}} = 0.9843$$
$$+ 0.398\varphi_{\text{p}}^{0.7383}\left(\frac{1}{d_{\text{p}}}\right)^{0.2246}\left(\frac{\mu_{\text{eff}}(T)}{\mu_{\text{f}}(T)}\right)^{0.0235} - 3.9517\frac{\varphi_{\text{p}}}{T}$$
$$+ 34.034\frac{\varphi_{\text{p}}^2}{T^3} + 32.509\frac{\varphi_{\text{p}}}{T^2} \tag{1}$$

where $0 \leq \varphi_p \leq 10\%$, 11 nm $\leq d_p \leq 150$ nm, 20 °C $\leq T \leq 70$ °C. This correlation was tested with experimental data [16, 55, 56], and results were in good agreement.

$$\mu_{\text{eff}} = -0.4491 + \frac{28.837}{T} + 0.574\varphi_{\text{p}} - 0.1634\varphi_{\text{p}}^2$$
$$+ 23.053\frac{\varphi_{\text{p}}^2}{T^2} + 0.0132\varphi_{\text{p}}^3 - 2354.735\frac{\varphi_{\text{p}}}{T^3}$$
$$+ 23.498\frac{\varphi_{\text{p}}^2}{d_{\text{p}}^2} - 3.0185\frac{\varphi_{\text{p}}^3}{d_{\text{p}}^2} \tag{2}$$

where $1\% \leq \varphi_{\text{p}} \leq 10\%$, 13 nm $\leq d_p \leq 131$ nm, 20 °C $\leq T \leq 70$ °C. This correlation was proven in line with results from past studies [46, 57–59].

On the other side, the effect on Nusselt number using different thermal conductivity models was numerically compared by Ogut and Kahveci [60] in 2016. Nusselt number of Al$_2$O$_3$–water/ethylene glycol nanofluid was analyzed in a square enclosure with lid-driven. Four models studied were Pak and Cho model [46], Yu and Choi model [44], Ghanbarpour et al. model [61], Maxwell model [42], and Timofeeva et al. [62] model. Among all models, Pak and Cho model gave the highest average number of Nusselt number. Noted that *M3* in two graphs shown below is Pak and Cho model (Fig. 4).

In short, each model has different considerations on different aspects, and thus, many modified models and new correlations were proposed by former researchers specifically for certain nanoparticles and working parameters. Some of the earliest models, modified models and correlations adopted are summarized in Table 2, with additional information obtained from the past study [63].

Artificial neural network (ANN) modeling in predicting thermophysical properties

Not only traditional method can be used to measure thermophysical properties, but artificial neural network (ANN) is able to present experimental data in shorter time and even more accurate than existing mathematical model. It simulates human brain neural network as artificial neurons
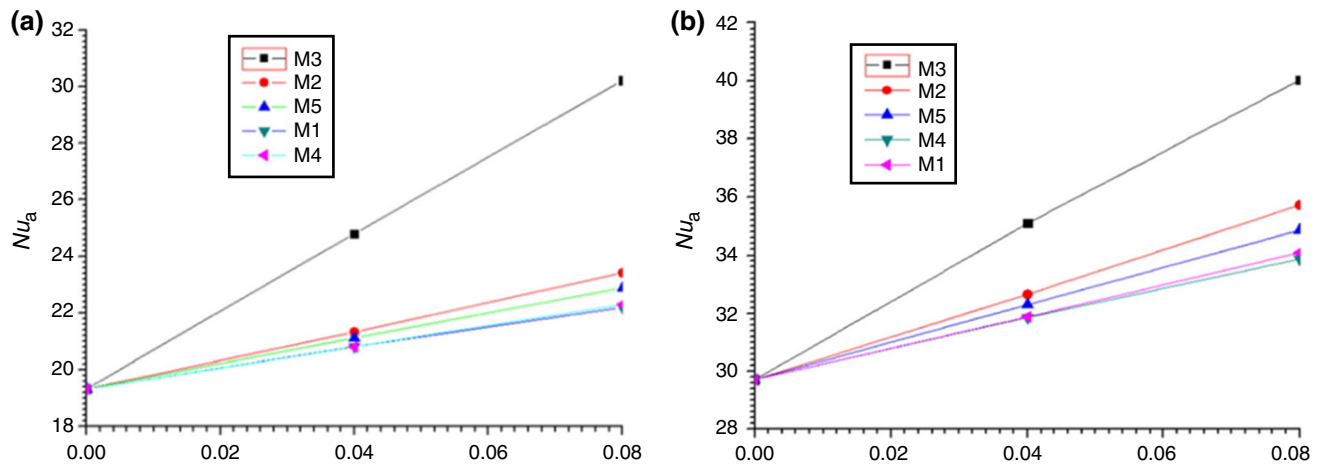
Fig. 4 Average Nusselt number for **a** 0:100% and **b** 40:60% ethylene glycol/water mixture (License Number: 4344041420177)

in data processing. Artificial neurons are made up of different artificial neurons in which each unit represents specified input, computation/function and output [79] (Fig. 5).

Hemmat et al. [80] determined thermal conductivity of hybrid nanofluid using transient hot-wire method with KD2 Pro conductivity meter. Firstly, MWCNTs with inner diameter of 3–5 nm and outer diameter of 5–15 nm were mixed with 10–30 nm ZnO nanoparticles and water/ethylene glycol mixture. Thermal conductivity was then measured from 0.02 to 1 vol%. Among the collected results, maximum thermal conductivity (TCR) was obtained at concentration of 1 vol% and temperature of 50 °C. Their proposed correlation and ANN were able to provide maximum error of 97.4 and 98%, and R-squared value of 0.9864 and 0.9968, respectively, in predicting TCR.

Thermal conductivity of CuO–single-walled carbon nanotubes (SWCNTs) dispersed in water/ethylene glycol was investigated by Rostamian et al. [79]. Temperature was altered from 20 to 50 °C, and nanoparticles concentration ranged from 0.02 to 0.75 vol%. They found that concentration variation was more dominant than operating temperature in thermal conductivity increment. Moreover, ANN gave more precise and accurate answer than their proposed correlation to estimate thermal conductivity of the hybrid nanofluid as maximum deviation of ANN and correlation was 0.544 and 4%, respectively.

Zhao and Li [81] predicted the thermal conductivity and viscosity of alumina–water nanofluid using ANN-RBF (radial basis function) model. Four different concentrations (1.31, 2.72, 4.25 and 5.92%) of nanofluids were prepared. Within 296–313 K, the ANN-RBF model has been having mean absolute percent error of 0.5177 and 0.5168% to estimate thermal conductivity and viscosity. Their finding showed that viscosity was mainly dependant on Al_2O_3 concentration, whereas thermal conductivity relies on both

nanoparticles concentration and temperature. Esfe et al. [82] used ANN model to predict thermal conductivity and viscosity of ferromagnetic–ethylene glycol nanofluid. Total of 72 experimental data were compared with ANN model, and the outcome showed 2 and 2.5% maximum error in the prediction of thermal conductivity and viscosity, respectively.

For hybrid Fe_2O_3/MWCNT nanofluid, Chen et al. [32] varied the concentration of Fe_2O_3 nanoparticles and measured the thermal conductivity. With 0.02 mass% Fe_2O_3 and 0.05 mass% MWCNT, they obtained 27.7% of enhancement in thermal conductivity. However, when they added more Fe_2O_3 (> 0.02 mass%) in the hybrid suspension, thermal conductivity decrement was observed. They proposed that high concentration of nanoparticles would lead to agglomeration easily, in which affecting heat transfer performance significantly.

It can be seen that most of the former researchers reported enhanced thermal conductivity and viscosity when nanofluid was used. When concentration of nanoparticles is increased, both thermophysical properties increase as well. The behavior of nanoparticles in improving base fluid is favorable to elevate current systems from various applications. Although higher concentration of nanoparticles can show more improvement and more efficient than conventional fluid, excessive amount of nanoparticles can still corrupt thermal conductivity which directly affects heat transfer performance [83].

Engine cooling and vehicle radiator system

For few decades till today, vehicle engine system is becoming more advanced due to men's incessant pursue of higher-performance engines. However, heat generated from engine block system is a huge drawback on overall

Table 2 Models used to compute thermophysical properties

Thermophysical property	Equation	Model
Thermal conductivity	$\frac{k_{nf}}{k_f} = \frac{k_{np} + 2k_f + 2\left(k_f - k_{np}\right)\varphi}{k_{np} + 2k_f - \left(k_f - k_{np}\right)\varphi}$	Maxwell model [42]
	$\frac{k_{nf}}{k_f} = -0.845 + 0.145e\left(2.43\varphi^{0.0637}\right)\varphi^{-0.11}T^{0.0673}$	Shamaeil et al. [64]
	$\frac{k_{nf}}{k_f} = \frac{k_{np} + (n-1)k_f - (n-1)\left(k_f - k_{np}\right)\varphi}{k_{np} + (n-1)k_f + \left(k_f - k_{np}\right)\varphi}$	Hamilton and Crosser [43]
	$\frac{k_{nf}}{k_f} = \frac{k_p + 2k_f - 2\varphi\left(k_f - k_{np}\right)(1+\eta)^3}{k_p + 2k_f + \varphi\left(k_f - k_{np}\right)(1+\eta)^3}$	Yu and Choi [44]
	$\frac{k_{nf}}{k_f} = \left[1 + \frac{k_{np}\varphi d_f}{k_f(1-\varphi)d_{np}}\right]$	Eastman et al. [65]
	$\frac{k_{nf}}{k_f} = 1 + 3\varphi$	Timofeeva et al. [62]
	$\frac{k_{nf}}{k_f} = 1.72\varphi + 1.0$	Mintsa et al. [55]
	$\frac{k_{nf}}{k_f} = 1 + \frac{k_{np}\varphi d_f}{k_f(1-\varphi)d_{np}}\left[1 + c\frac{2k_B T d_{np}}{\pi \alpha_f \mu_f d_{np}^2}\right]$	Patel et al. [66]
	$\frac{k_{nf}}{k_f} = \frac{k_{np} + 2k_f - 2\varphi\left(k_f - k_{np}\right)}{k_{np} + 2k_f + \varphi\left(k_f - k_{np}\right)}\left(1 + b\varphi Pe_{np}^m\right)$	Charuyakorn et al. [67]
	$\frac{k_{nf}}{k_f} = 1 + 64.7\varphi^{0.764}\left(\frac{d_f}{d_{np}}\right)^{0.369}\left(\frac{k_f}{k}\right)^{0.7476}Pr_T Re_T^{1.2321}$	Chon et al. [68]
	$\frac{k_{nf}}{k_f} = \frac{k_{np} + 2k_f - 2\varphi\left(k_f - k_{np}\right)}{k_{np} + 2k_f + \left(k_f - k_{np}\right)\varphi}$	Wasp et al. [69]
	$k_{nf} = k_f\left[\frac{k_{np} + 2k_f - 2\varphi\left(k_f - k_{np}\right)}{k_{np} + 2k_f - \left(k_f - k_{np}\right)\varphi}\right] + 5\times10^4\beta\varphi\rho_f\left(C_p\right)\sqrt{\frac{k_B T}{d_{np}\rho_{np}}}f(T,\varphi),$ where $f(T,\varphi) = (-6.04\varphi + 0.4705)T + (1722.3\varphi - 134.63)$	Koo and Kleinstreuer [45]
	$\frac{k_{nf}}{k_f} = 1 + 3.5\varphi + 2.5\varphi^2$	Ghanbarpour et al. [61]
	$\frac{k_{nf}}{k_f} = 1 + 4.4Re^{0.4}Pr^{0.66}\left(\frac{T_f}{T_{fr}}\right)^{10}\left(\frac{k_{np}}{k_f}\right)^{0.03}\varphi^{0.66}$	Corcione [48]
	$\frac{k_{nf}}{k_f} = 4.97\varphi^2 + 2.72\varphi + 1$, for water–$\gamma Al_2O_3$ $\frac{k_{nf}}{k_f} = 28.905\varphi^2 + 2.8273\varphi + 1$, for ethylene glycol-$\gamma Al_2O_3$	Maiga et al. [47]
	$\frac{k_{nf}}{k_f} = 1 + 7.47\varphi$	Pak and Cho [46]
	$k_{hnf} = k_f\frac{\frac{\left(\varphi_{np1}k_{np1} + \varphi_{np2}k_{np2}\right)}{\varphi_{hnf}} + 2k_f + 2\left(\varphi_{np1}k_{np1} + \varphi_{np2}k_{np2}\right) - 2\varphi k_f}{\frac{\left(\varphi_{np1}k_{np1} + \varphi_{np2}k_{np2}\right)}{\varphi_{hnf}} + 2k_f - 2\left(\varphi_{np1}k_{np1} + \varphi_{np2}k_{np2}\right) + \varphi k_f}$	Takabi et al. [70]
	$\frac{k_{hnf}}{k_f} = 1 + 0.0162\varphi^{0.7038}T^{0.6009}$ *For MWCNT–Fe_3O_4/EG	Saeed Sarbolookzadeh Harandi et al. [71]
	$\frac{k_{hnf}}{k_f} = 0.8341 + 1.1\varphi^{0.243}T^{-0.289}$ *For MgO–FMWCNT/EG	Masoud Afrand [72]
Dynamic viscosity	$\mu_{nf} = \mu(1 + 2.5\varphi)$ where $\varphi < 0.05$	Einstein [49]
	$\mu_{nf} = \left(1 + 2.5\varphi_{np} + 6.2\varphi_{np}^2\right)\mu_f$	Batchelor [50]
	$\frac{\mu_{nf}}{\mu_f} = \frac{1}{1 - 34.87\left(\frac{d_{np}}{d_f}\right)^{-0.3}\varphi^{1.03}}$	Corcione [48]
	$\frac{\mu_{nf}}{\mu_f} = 123\varphi^2 + 7.3\varphi + 1$ $\frac{\mu_{nf}}{\mu_f} = 306\varphi^2 - 0.19\varphi + 1$	Maiga et al. [47]
	$\frac{\mu_{nf}}{\mu_f} = \frac{1}{(1-\varphi)^{2.5}}$	Brinkman [73]
	$\frac{\mu_{nf}}{\mu_f} = 1 + 2.5\varphi + 4.698\varphi^2$	De Bruijin [74]
	$\frac{\mu_{nf}}{\mu_f} = 1 + 2.5\varphi + \left[3.125 + \left(\frac{2.5}{\varphi_{max}}\right)\right]\varphi^2$	Mooney [75]
	$\frac{\mu_{nf}}{\mu_f} = \left(1 + 1.5\varphi_p\right)e^{\frac{\varphi_p}{1-\varphi_m}}$	Nielsen [76]
	$\frac{\mu_{nf}}{\mu_f} = 1 + 7.3\varphi + 123\varphi^2$	Wang et al. [15]
	$\frac{\mu_{nf}}{\mu_f} = 0.904e^{14.8\varphi}$	Gherasim et al. [51]

Table 2 continued

| Thermophysical property	Equation	Model
	$\frac{\mu_{nf}}{\mu_f} = \frac{1}{1-34.87\left(\frac{d_{np}}{d_f}\right)^{-0.3}\varphi^{1.03}}$ where $d_f = \left[\frac{6M}{N\pi\rho b_f}\right]^{\frac{1}{3}}$	Tiwari and Das [52]
	$\frac{\mu_{hnf}}{\mu_f} = [0.191\varphi + 0.240(T^{-0.342}\varphi^{-0.473})]\exp\left(1.45T^{0.120}\varphi^{0.158}\right)$	Omid Soltani and Mohammad Akbari [77]
	*For MgO–MWCNT/EG	
	$\mu_{hnf} = 328201 \times T^{-2.053} \times \varphi^{0.09359}$	Asadi et al. [78]
	*For MWCNT–MgO/engine oil	
Density	$\rho_{eff} = \left(\frac{m}{V}\right)_{eff} = \frac{m_f+m_{np}}{v_f+v_{np}} = \frac{\rho_f V_f + \rho_{np} V_{np}}{v_f+v_{np}} = \left(1-\varphi_{np}\right)\rho_f + \varphi_{np}\rho_{np}$	Pak and Cho [46]
	$\rho_{eff} = 1001.064 + 2738.6191\varphi_{np} - 0.2095T$	Khanafer and Vafai [53]
	$\rho_{hnf} = \varphi_{np1}\rho_{np1} + \varphi_{np2}\rho_{np2} + \left(1-\varphi_{np1+np2}\right)\rho_f$	Takabi et al. [70]
Specific heat capacity	$\left(C_p\right)_{nf} = (1-\varphi)\left(c_p\right)_f + \varphi\left(c_p\right)_{np}$	General equation
	$\left(C_p\right)_{nf} = \frac{\left(1-\varphi_{np}\right)\rho_f\left(c_p\right)_f + \varphi_{np}\rho_p\left(c_p\right)_{np}}{\rho_{nf}}$	Pak and Cho [46]
	$\left(C_p\right)_{hnf} = \frac{\left(1-\varphi_p\right)\rho_f\left(c_p\right)_f + \varphi_{np1}\rho_{np1}\left(c_p\right)_{np1} + \varphi_{np2}\rho_{np2}\left(c_p\right)_{np2}}{\rho_{hnf}}$	Takabi et al. [70]
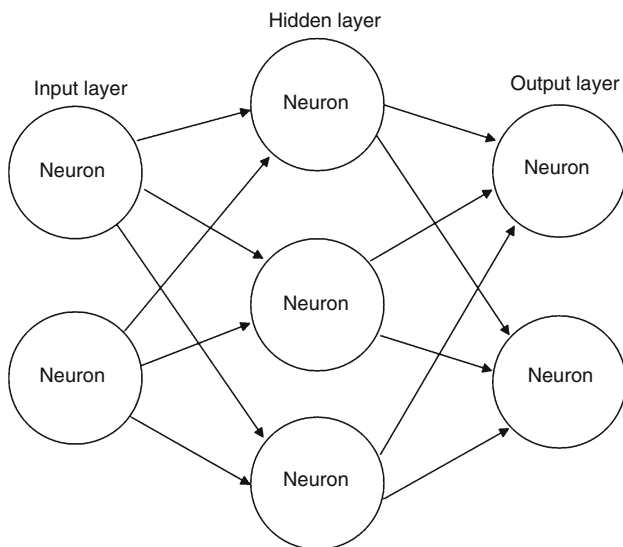
Fig. 5 Concept diagram of ANN

performance. In a car engine cooling system, coolant is initially pumped into engine block system from radiator via flowing tube. Then, the coolant absorbs heat generated from the engine block which mainly results from friction due to the movement of pistons to turn the crankshaft for rotating vehicle wheels. Engine blocks are usually made up of cast iron or aluminum alloy. After that, coolant flows to radiator when it reaches certain temperature by triggering thermostat. Thermostat is located between engine block system and radiator. It acts as a valve to regulate the coolant flowing to radiator so temperature of the engine block system can be controlled. The mechanism behind it

is that the wax at the thermostat melts when the temperature reaches its preset value and a rod connecting to the valve will be pushed away due to thermal expansion of wax and then opening the valve. Before hot coolant enters radiator, the high temperature may cause high pressure in the flowing tube and expansion tank with cap or pressure regulating valve is used to release the excessive pressure. At the last stage, hot coolant flowing inside the radiator will be cooled by surrounding air with the aid of fan behind the radiator (Fig. 6).

Failure of efficient heat transfer could lead to overheating of engine and next damaging engine block body. Thus, maintaining temperature of engine block system is crucial to strengthen its life span and performance. Radiator acts as heat exchanger in vehicle cooling system to transfer heat away from the engine block system to surrounding. In order to attract more users, many improvements have been done by engine companies on radiator system since back then, such as adding fins to increase surface area, changing radiator material and using different configuration of tubes (cross flow, counter flow, parallel flow and shell-and-tube). Nonetheless, there are limitations on these renovations in which few consequences have to be taken into consideration: size of radiator, burden on car, cost of material, durability of material and more.

In the history of development, water was first used as coolant in vehicle cooling system. In some countries with extremely cold weather, water tends to freeze and causes damage to flowing tubes and engine block due to its volume expansion. Then, antifreeze agent was introduced as additive to make up deficiencies of water which has unsatisfying freezing point and low boiling point. Advantage of increasing boiling point is that coolant is allowed to

Fig. 6 Automobile engine
cooling system
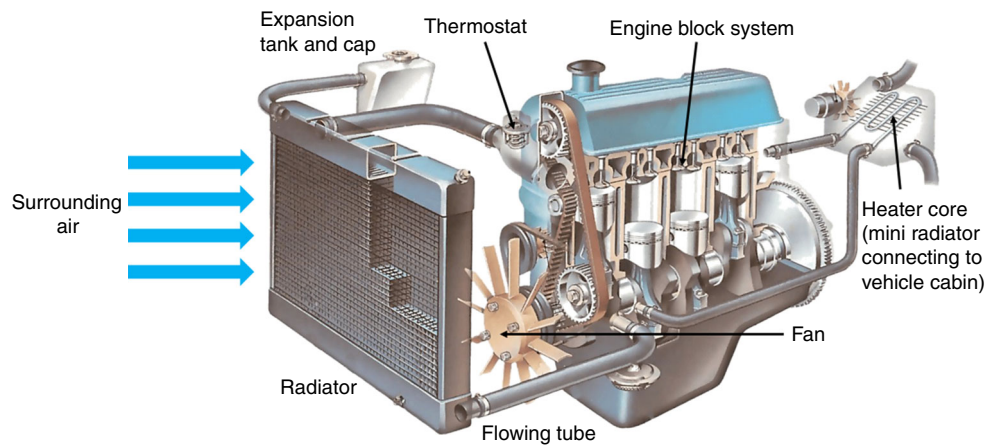
absorb more heat to reach higher operating temperature;
thus, more heat can be rejected in a cycle, which mean
higher power engine can be implemented. Nowadays,
water/ethylene glycol mixture is used as conventional
automobile coolant because water and ethylene glycol
alone are poor heat transfer fluid. Table 3 and Fig. 7 show
the properties of water, ethylene glycol and water/ethylene
glycol mixture.

According to comprehensive review from Saidur et al.
[84], thermal conductivity is one of the main factors which
contribute to the enhancement of heat transfer performance

in various applications. Up to authors' literature review,
implantation of nanofluid into vehicle cooling system was
initiated by Choi et al. [85] in 2001. They measured ther-
mal conductivity of metal and oxide nanofluids produced
themselves. It was found that the measured values were
much higher than expected values, and they proposed that
nanofluid could enhance vehicle thermal performance. This
has led former researchers to start exploring the superior
performance of nanofluid as coolant in automobile cooling
system.

Table 3 Properties of water and
ethylene glycol

	Water	Ethylene glycol
Density/kg m^{-3}	997	1113
Freezing point/°C	0	-12.9
Boiling point/°C	100	197.3
Viscosity/N s m^{-2}	1.002×10^{-3}	0.162×10^{-1}
Thermal conductivity/W m^{-1} K^{-1}	0.609	0.258

Fig. 7 Boiling and freezing
points result from ratio of
ethylene glycol to water
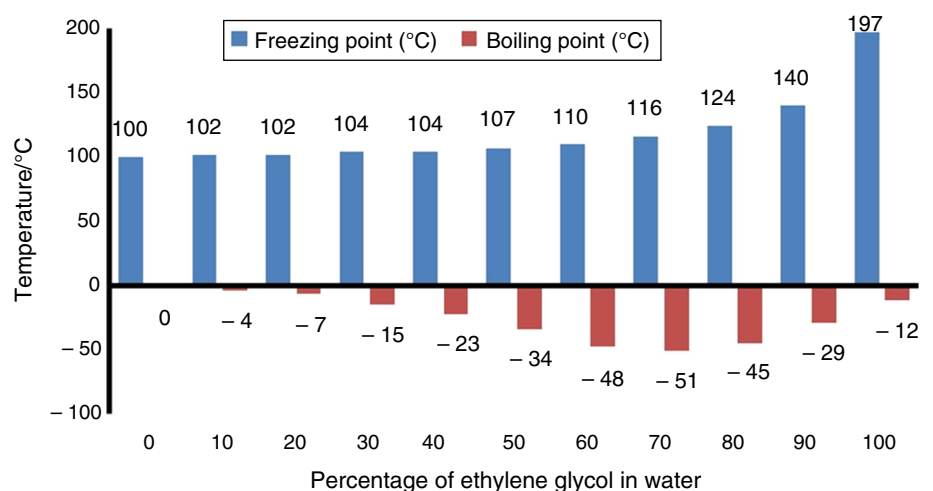
Experimental studies on nanofluid in automobile radiator cooling system

In order to determine the thermal and flow performance of nanofluids in automobile radiator, many test rigs were set up and studied based on the actual condition of engine radiator system. Non-oxide ceramic material, SiC, was first dispersed into automobile engine coolant by Li et al. [38] to investigate its thermal conductivity. At 50 °C, 0.5 vol% of SiC nanoparticles could enhance thermal conductivity up to 53.81%. For 0.2 vol% concentration, it was found that the overall effectiveness achieved about 1.6, which means that it could act as better engine coolant than conventional water/ethylene glycol.

Selvam et al. [6] investigated the amount of enhancement by dispersing graphene nanoplatelets into water/ethylene glycol mixture in a louvered fin flat tube. Their results revealed that the combination of these parameters, namely nanoparticle concentration (0.5 vol%), nanofluid flow rate (62.5 g s^{-1}) and ambient air velocity (5 m s^{-1}), contributed to about 104 and 81% of enhancement at inlet temperatures of 35 and 45 °C, respectively. In the same year, Selvam and his team [86] seek to deepen the understanding on the performance of the same nanofluid and tube. From the obtained results, they strengthen the statement from their previous work in which mass flow rate of nanocoolant was more dominant than nanoparticle concentration in the increment of pressure drop. For convective heat transfer coefficient, 51 and 20% of improvement were found at 45 and 35 °C, respectively, with nanoparticle concentration of 0.5% and mass flow rate of 100 g s^{-1}.

Islam et al. [7] investigated the effects of nanocoolant used in a 2.4-kW Proton Exchange Membrane Fuel Cell. ZnO was chosen as working nanoparticle due to its better stability and low electrical conductivity compared to Al_2O_3 and TiO_2. From their observation, using 0.5 vol% ZnO nanocoolant enhanced the cooling performance by 29%, reduction in radiator size by almost 27% and increment of less than 10% in pumping power.

Azmi et al. [8] investigated heat transfer performance of water/ethylene glycol nanofluid containing TiO_2 under turbulent flow in a circular tube. Compared to base fluid, the nanofluid showed 28.9% of enhancement at 70 °C when concentration of TiO_2 was increased from 0.5 to 1.5 vol%. The team developed correlations for Nusselt number, and friction factor and the average error were 4.9 and 3.3%, respectively. Then, Azmi and his co-workers [87] compared the convective heat transfer coefficient of Al_2O_3 and TiO_2 dispersed in water/ethylene glycol (60:40) mixture. Three different operating temperatures were considered, and it was found that at 30 °C, heat transfer coefficient of Al_2O_3 has higher value than TiO_2 nanofluids.

Meanwhile at 70 °C, Al_2O_3 and TiO_2 nanofluids showed 23.8 and 24.2% of heat transfer enhancement at 1 vol% of concentration compared to base fluid.

Using a flat tube radiator, Alosious et al. [88] conducted experimental and numerical study on the hydrodynamic and heat transfer performance of two water-based nanofluids mixed with Al_2O_3 and CuO nanoparticles. Both prepared nanoparticles having diameter of less than 50 nm, 0.05 vol% concentration, forced to flow within $136 < Re < 186$ and fixed inlet temperature of 90 °C. On the other side, Reynolds number range remained the same, but volume concentration was varied from 0.05 to 1% in numerical study. From their experimental outcome, Al_2O_3 and CuO nanofluids contributed 0.5 and 0.38% of enhancement in overall heat transfer coefficient, respectively. Result obtained from the numerical study showed that 1% of volume concentration of CuO and Al_2O_3 nanofluids at Reynolds number equal to 816 led to 13.2 and 16.4% of heat transfer coefficient improvement, respectively. For the same amount of heat released by water, 1 vol% CuO and Al_2O_3 could reduce the area of radiator by 2.1 and 2.9%. Lastly, they suggested that volume concentration of 0.4–0.8% was the optimum value where pumping power could be neglected.

Goudarzi and Jamali [89] tested the effect when both nanofluid and wire coil insert were used in a car cooling system. Different amounts of Al_2O_3 nanoparticles were dispersed in ethylene glycol to produce three different concentrations (0.08, 0.5 and 1%) of nanofluids. The copper wire coil inserts have been having 1.3 cm width and 0.3 mm thickness. Up to 9% of heat transfer augmentation was reported for using wire coil inserts, and when nanofluid was used together with the inserts, the effect boosted for 5% more.

The consequences of implementing CuO–water nanofluid in a four-stroke diesel engine were identified by Senthilraja et al. [90]. For 0.05, 0.1 and 0.2% CuO nanoparticles concentration, specific fuel consumption was reduced by 8.6, 15.1 and 21.1%, followed by emission of NO_x at 881, 853 and 833 ppm, respectively. At the same time, Muruganandam and Kumar [91] tested MWCNT–water nanofluid as coolant used in four-stroke diesel engine as well. As a result, exhaust temperature was decreased by 10% and brake thermal efficiency was increased by 15%.

Effectiveness of MWCNT nanofluid in an air-cooled radiator was determined by Oliveira and his party [92]. The constant parameter in the experiment was air flow rate of 0.175 kg s^{-1} and four inlet temperatures from 50 to 80 °C. Hot fluid which was to be cooled by air was varied from 30 to 70 g s^{-1}. Viscosity was increased for 54% at 30 °C and 0.16 mass% concentration. However, heat transfer deterioration was observed at 0.16 mass% MWCNT as distilled water presented higher heat transfer rate.

Water-/ethylene glycol-based alumina nanofluid was adopted by Gulhane and his partner [93]. The parameters altered were nanoparticle concentration (0.1–0.4 vol%), flow rate (2–5 L min^{-1}) and inlet temperature (50, 60 and 70 °C). When compared to base fluid, 45.87% of enhancement in heat transfer coefficient was acquired, due to increased nanoparticles concentration. Their explanations were consistent with those made by Sheikhzadeh et al. [94] who worked on the same nanofluid but different parameter values. Laminar flow was considered by setting 9, 11 and 13 L min^{-1} for volume concentration of 0.003–0.012%. At 13 L min^{-1}, 0.012 vol% alumina nanofluid raised Nusselt number for about 9%. Likewise, empirical correlation for Nusselt number developed was able to do prediction with 3% maximum error.

Some researchers reported heat transfer enhancement of adding TiO_2 in water/ethylene glycol. Chen and Jia [17] varied the nanoparticle concentration from 0.5 to 5 and 10% of improvement was observed. Jagadishwar and Sudhakar [95] prepared the nanofluid in 0.1, 0.2 and 0.35% concentration and evaluated from 6 to 16 L min^{-1}. Their product showed heat transfer inclination of 42.5% with only 0.35% of TiO_2. Using the same base fluid and coolant flow rate, Kumar and Appalanaidu [96] dispersed ZnO and tested with inlet temperature of 50–80 °C. Surprisingly with the similar result, 0.4 vol% of ZnO brought up the enhancement of heat transfer rate to 46% when compared to base fluid.

γ-Al_2O_3/water nanofluid was experimentally studied by Moghaieb et al. [97]. Diameter of nanoparticles ranged from 21 to 37 nm. Four parameters were taken into consideration: nanoparticles concentration (0–2 vol%), coolant flow velocity (1–2 m s^{-1}), heat flux (100–400 kW m^{-2}) and bulk temperature (60–80 °C) in experiment. From their inspection, maximum heat transfer coefficient of 78.67% was reported at 1 vol%, 80 °C and 2 m s^{-1} when compared to water. Convective heat transfer coefficient decreased with increasing coolant temperature and increased with coolant flow velocity.

Heat transfer enhancement of bioglycol that has higher boiling point and lower freezing point was mixed with water and TiO_2 nanoparticles. Abdolbaqi and his squad [98] tested the nanofluid in a flat tube under constant heat flux. Authors had reported augmentation of Nusselt number for about 28.2% when compared to water. Surprisingly, decline of Nusselt number was about 3% at 2.0 vol% TiO_2 and 30 °C operating temperature. Also, friction factor increased by 6.1 and 14.3% at 1.0 and 2.0 vol% nanoparticles.

Sajedi et al. [99] in 2016 suggested that ignoring hydraulic effect might cause miscalculation in heat transfer performance of nanofluid when compared to base fluid. In their experimental setup, pumping power and Reynolds number were fixed for turbulent flow in a finned air-cooled heat exchanger. Three different concentrations (0.5, 1 and 2.5%) were compared at different temperatures. In their analysis, maximum difference of 15% was obtained for 2.5 vol% SiO_2 in water base fluid and 40 °C operating temperature. Based on their result, they concluded that considering constant pumping power as criteria for computing heat transfer performance is appropriate instead of constant Reynolds number.

Experimental studies above are summarized in Table 4, and some other studies are included as well.

Experimental studies on various types of automobile radiator

Heat exchangers are broadly utilized in various engineering applications, such as waste heat recovery, air-conditioning system, refrigerator, automobile cooling system, chemical and food industries [107]. Heat exchanger installed in vehicle is usually called as radiator. Generally, there are many types of radiators used in automobile engine cooling system: parallel flow, counter flow, cross flow and shell-and-tube heat exchanger. However, different configurations of heat exchangers are still limited by durability of material, in which restricted high thermal performance and compactness of radiator. Thus, former researchers studied on performance of nanofluids flowing in different types of heat exchangers, and the outcome is tabulated in Table 5.

Experimental studies using real vehicle engine

One of the earliest experimental studies using actual vehicle components was carried out by Tzeng et al. [124]. His team determined the heat transfer performance of transmission oil with the addition of CuO, Al_2O_3 and antifoam in a four-wheel-drive (Mazda brand) transmission system. The experiment was carried out at four different rotating speeds, starting from 400 to 1600 with 400 rpm increment for each interval. Their result reported that CuO had the best heat transfer performance at both high and low rotating speeds because its distribution of temperature was the lowest one. Two years later, Zhang and his colleagues [125] tested the performance of heavy-duty-diesel engine by adding 3% concentration of nanographite into coolant. It was found that the cooling capability of the nanocoolant was 15% higher than the original coolant itself.

In 2014, radiator from Toyota Yaris 2007 was used to identify the forced convection heat transfer of Al_2O_3 nanofluid by Ali et al. [126]. The nanofluid was prepared with different volume concentrations: 0.1, 0.5, 1.0, 1.5 and 2%. Their finding showed that the optimum heat transfer coefficient was found at 1% volume concentration and heat transfer deterioration occurred when the concentration was

Table 4 Summary of experimental studies of nanofluid in automobile cooling system

Authors	Nanofluid	Findings
Li et al. [38]	SiC–water/ethylene glycol (EG)	With 0.2 vol% concentration SiC, overall effectiveness achieved about 1.6 at 50 °C
Selvam et al. [6]	Graphene–water/EG	0.5 vol% graphene with flow rate of 62.5 g s^{-1} and ambient air velocity (5 m s^{-1}) contributed to about 104 and 81% of heat transfer coefficient enhancement at inlet temperature of 35 °C and 45 °C, respectively
Selvam and his team [86]	Graphene–water/EG	For convective heat transfer coefficient, 51 and 20% of improvement were 45 and 35 °C, respectively, with 0.5 vol% graphene and mass flow rate of 100 g s^{-1}
Islam et al. [7]	ZnO–water/EG	0.5 vol% ZnO nanocoolant enhanced the cooling performance by 29% and increment of less than 10% in pumping power. Radiator size can be cut down by almost 27%
Azmi et al. [8]	TiO$_2$–water/EG	Compared to base fluid, 1.5 vol% TiO$_2$ showed 28.9% of heat transfer enhancement at 70 °C
Azmi and his co-workers [87]	Al$_2$O$_3$ and TiO$_2$–water/EG (60:40)	At 70 °C, Al$_2$O$_3$ and TiO$_2$ nanofluids showed 23.8 and 24.2% of heat transfer enhancement at 1 vol% of concentration when compared to base fluid
Alosious et al. [88]	Al$_2$O$_3$ and CuO–water	Al$_2$O$_3$ and CuO nanofluids contributed 0.5 and 0.38% of enhancement in overall heat transfer coefficient, respectively. Both prepared nanoparticles having diameter of less than 50 nm, 0.05 vol% concentration, forced to flow within $136 < Re < 186$ and fixed inlet temperature of 90 °C
Goudarzi and Jamali [89]	Al$_2$O$_3$–EG	Using wire coil inserts caused 9% heat transfer augmentation, and when nanofluid was added, the effect boosted for 5% more
Senthilraja et al. [90]	CuO–water	For 0.05, 0.1 and 0.2% CuO nanoparticles concentration, specific fuel consumption for four-stroke diesel engine was reduced by 8.6, 15.1 and 21.1%, respectively
Muruganandam and Kumar [91]	MWCNT–water	Exhaust temperature was decreased by 10%, and brake thermal efficiency was increased by 15% for four-stroke diesel engine
Oliveira and his party [92]	MWCNT–water	Heat transfer deterioration was observed at 0.16 mass% MWCNT
Gulhane and his partner [93]	Al$_2$O$_3$–water/EG	Increasing nanoparticles concentration from 0.1 to 0.4 vol%, heat transfer coefficient enhanced for 45.87% when compared to base fluid
Sheikhzadeh et al. [94]	Al$_2$O$_3$–water/EG	At 13 L min^{-1}, 0.012 vol% alumina nanofluid raised Nusselt number for about 9%
Jagadishwar and Sudhakar [95]	TiO$_2$–water/EG	0.35% of TiO$_2$ enhanced heat transfer for 42.5%
Chen and Jia [17]	TiO$_2$–water/EG	Varying nanoparticle concentration from 0.5 to 5% caused heat transfer improved for 10%
Kumar and Appalanaidu [96]	ZnO–water/EG	0.4 vol% of ZnO brought up the enhancement of heat transfer rate to 46% when compared to base fluid
Moghaieb et al. [97]	γ-Al$_2$O$_3$–water	Maximum heat transfer coefficient of 78.67% was reported at 1 vol%, 80 °C and 2 m s^{-1} when compared to water
Abdolbaqi and his squad [98]	TiO$_2$–water/bioglycol	Declination of Nusselt number was about 3% at 2.0 vol% TiO$_2$ and 30 °C operating temperature
Sajedi et al. [99]	SiO$_2$–water	Considering constant pumping power for computing heat transfer performance is more appropriate
Azmi et al. [100]	Al$_2$O$_3$–water/EG (60:40, 50:50 and 40:60)	Nanofluid with 60:40 base fluid ratio showed highest HTC enhancement (24.6%) at 1 vol% Al$_2$O$_3$
Yu et al. [101]	Al$_2$O$_3$–water/EG (55:45)	1.0 and 2.0 vol% Al$_2$O$_3$ increased heat transfer coefficient by 57 and 106%, respectively, compared to base fluid
Naraki et al. [102]	CuO–water	Heat transfer coefficient was enhanced from 6 to 8% when CuO volume concentration was varied from 0.15 to 0.4%
		When inlet temperature was increased from 50 to 80 °C, overall heat transfer coefficient decreased
Ebrahimi et al. [103]	SiO$_2$–water	0.4 vol% SiO$_2$ generated maximum heat transfer enhancement of 9.3% at 60 °C.
Hussein et al. [104]	SiO$_2$–water	Heat transfer enhanced from 39 to 56% when concentration of SiO$_2$ was increased from 1 to 2.5 vol%
Chougule and Sahu [37]	Al$_2$O$_3$–water CNT–water	Al$_2$O$_3$ and CNT nanofluid with 1.0 vol% showed maximum heat transfer performance of 90.76 and 52.03%, respectively
Heris et al. [105]	CuO–water/EG	0.8 vol% CuO showed enhancement of heat transfer coefficient for about 55%

Table 4 (continued)

Authors	Nanofluid	Findings
Sarkar and Tarodiya [106]	Cu–water/EG SiC–water/EG Al$_2$O$_3$–water/EG TiO$_2$–water/EG	Maximum heat transfer enhancement was 15.34, 14.33, 14.03 and 10.20% for SiC, Al$_2$O$_3$, TiO$_2$ and Cu, respectively, with 1.0 vol% for all nanoparticles

further increased. 14.72 and 9.51% of maximum increment were found for Nusselt number and heat transfer coefficient of the coolant, respectively.

M'hamed et al. [127] investigated heat transfer performance of a Proton Kelisa 1000 cc engine system. MWCNT was mixed with water/ethylene glycol base fluid and used as coolant in their study. From their results, it was found that the nanocoolant with 0.50% of volume concentration yielded about 196% of maximum heat transfer coefficient enhancement in laminar flow condition. In 2006, Devireddy et al. [128] used a car radiator which was commercially available to demonstrate the performance of TiO$_2$ at different concentrations. They obtained heat transfer improvement of 35% at 0.5 vol% TiO$_2$ and proposed that Brownian motion might be the main contributor to the enhancement instead of thermophysical properties.

Not only four-wheel car engine system has been studied till now, Mathivanan and his team [129] used Aprilia SXV 450 (motorcycle) engine in their experimental setup. Various nanoparticles were mixed separately with distilled water and compared to each other. The nanofluids prepared included 1–100 nm of MWCNT, Al$_2$O$_3$, SiC and TiC nanoparticles. At 1% of nanoparticle concentration, TiO$_2$ nanofluid dissipated heat the most among all tested nanofluids and showed 31.9% of better heat dissipation capacity than water at 3.5 GPM of flow rate.

Numerical studies on nanofluid in automobile radiator cooling system

Sahoo et al. [130] analyzed the capability of brine-based nanocoolant in wavy finned radiator. They compared the heat transfer performance between two different types of nanoparticles (Ag and Al$_2$O$_3$) mixed with propylene glycol and ethylene glycol. It was found that both Ag and Al$_2$O$_3$ nanofluids with propylene glycol performed better than Ag and Al$_2$O$_3$ nanofluids with ethylene glycol. Apart from that, size and pumping power required by radiator could be reduced up to about 4 and 25.5% when Ag–propylene glycol nanofluid was used instead of base coolant without nanoparticles.

Another numerical study using Fluent software was carried out by Vajjha et al. [131] on flat tubes of radiator. Al$_2$O$_3$ and CuO nanofluids with water/ethylene glycol were

compared. 10 vol% Al$_2$O$_3$ nanofluid increased average heat transfer coefficient for 94% and expected to decrease required pumping power by 82% when compared to base fluid. On the other side, 6 vol% CuO contributed 89% enhancement in heat transfer coefficient and could reduce pumping power up to 77% on the basis of same amount of heat transfer from base fluid. Four years later, Vajjha et al. [132] studied on the thermal performance of same nanofluids in radiator flat tubes with similar dimensions. Both Al$_2$O$_3$ and CuO nanofluids with 3 vol% concentration increased the average heat transfer coefficient for 36.6 and 49.7% at Reynolds number equal to 5500. As a result, Al$_2$O$_3$ nanofluid allowed more reduction in terms of pumping power compared to CuO nanofluid.

Few years later, researchers from China and Iran [133] examined on four different nanomaterials mixed with water/ethylene glycol. Their result showed good agreement with correlation from past researchers [131]. A 3D vehicle radiator flattened tube was modeled using ANSYS and analyzed using Fluent. Laminar flow (500–2000 Reynolds number) and different shapes (cylindrical, spherical, platelet and brick) of nanoparticles were tested. It was noticed that CuO and TiO$_2$ could transfer heat better than Fe$_3$O$_4$ and Al$_2$O$_3$. Besides that, nanoparticles shape with minimum and maximum Nusselt numbers can be arranged as spherical, brick, cylindrical and platelet accordingly.

Five different hybrid nanofluids were produced by Sahoo and Sarkar [134] using Al$_2$O$_3$ and five different nanoparticles in an experiment. 1 vol% nanoparticle water/ethylene glycol nanofluids were tested in a louvered fin radiator. The authors found that 0.5% Ag mixed with 0.5% Al$_2$O$_3$ gave the highest value in heat transfer rate, effectiveness and pumping power. Meanwhile, highest performance index was obtained from the combination of SiC and Al$_2$O$_3$. They computed that reduction in radiator size could reach 3.7% for constant coolant flow rate and heat transfer rate, whereas coolant flow rate can be decreased by 3.1% for fixed heat transfer rate and radiator size, when Ag hybrid nanofluid was compared to base fluid.

Leong and his team [135] examined heat transfer behavior of Cu–ethylene glycol nanofluid as coolant in flat tubes of a diesel engine (TBD 232V-12). From their research, variation of Reynolds number for air has more obvious effect on thermal performance of the radiator than

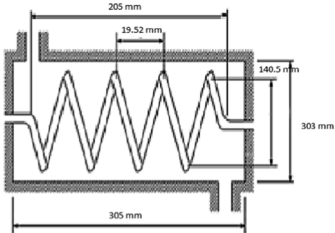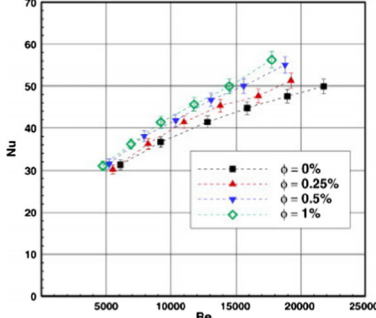**Table 5** Summary of performance of nanofluid in heat exchangers

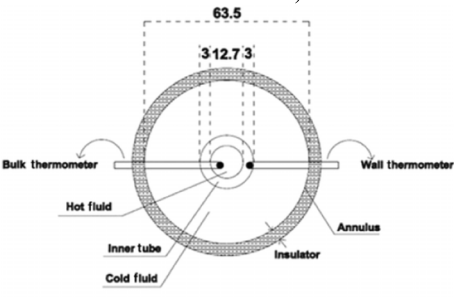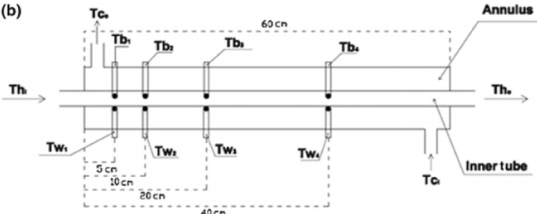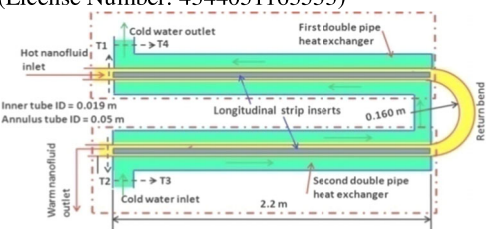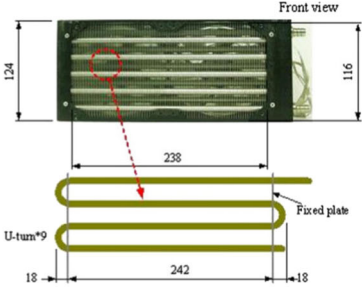| Type	Nanofluid	Finding
Shell and tube heat exchanger [108]	γ-Al_2O_3–water	Compared to water, the maximum increment of Nusselt number and overall heat transfer coefficient at 0.03, 0.14 and 0.3 vol% concentration of particles was around 9.7, 20.9, 29.8 and 5.4, 10.3, 19.1% respectively, when compared to base fluid
Shell and tube heat exchanger [109]	Al_2O_3 (20 nm) + water	For average heat transfer coefficient, 2 and 4% Al_2O_3 showed 5.42 and 11.94% enhancement. Incorporating nanoparticles into the base heating fluid of water could augment the effectiveness of the heat exchanger by 49%
Shell and coil heat exchanger [110] (License Number: 4344050355580)	γ-Al_2O_3 + water	When nanoparticle concentration increased, heat transfer enhancement increased as well. Heat transfer rate was proportional to mass flow rate but inversely proportional to fluid inlet temperature
Double pipe heat exchanger [111]	Aluminum Nitride-Ethylene Glycol	Hybrid nanofluid could drastically augment the thermal performances of heat exchanger by 35% in comparison with base fluid within temperature (25–50 °C) and concentrations (1–4 vol%)
Double pipe heat exchanger [112]	CuO + water	Within $5000 < Re < 18000$, when 0.05% CuO nanofluid replaced water in inner tube, convective heat transfer has improved. It was further enhanced with corrugations in inner pipe with penalty of pressure drop increased
Double tube heat exchanger [113] (License Number: 4345780140977) Inner tube internal diameter: 8.1 mm Inner tube external diameter: 9.57 mm Outer tube internal diameter: 150 mm Outer tube external diameter: – Test section length: 220 cm	Al_2O_3 (20 nm) + water	1 vol% of Al_2O_3 increased Nusselt number by maximum of 20% when compared to water
Double tube heat exchanger [114] Inner tube internal diameter: 8.13 mm Inner tube external diameter: 9.53 mm Outer tube internal diameter: 27.8 mm Outer tube external diameter: 33.9 mm Test section length: 150 cm	TiO_2 (21 nm) + water	26% of heat transfer coefficient enhancement was observed at 1.0 vol% TiO_2 whereas heat transfer coefficient was 14% lower than that of water at 2.0 vol% TiO_2

Table 5 continued
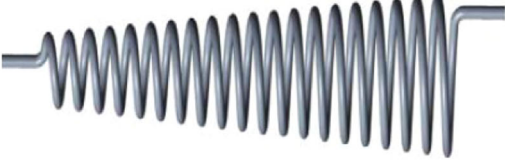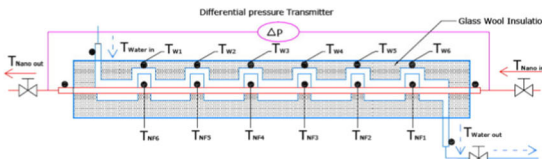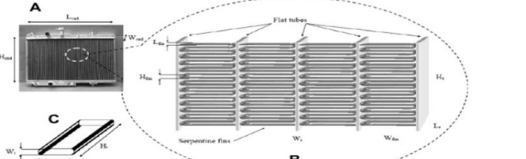
Double tube heat exchanger [115] Inner tube internal diameter: 6 mm Inner tube external diameter: 8 mm Outer tube internal diameter: 14 mm Outer tube external diameter: 16 mm Test section length: 120 cm	γ-Al_2O_3 (20 nm) + water	At mass flow rate equal to 60 g s^{-1}, heat transfer rate was increased by 7.32% with 0.2 vol% nanoparticles
Double tube heat exchanger [116] (License Number: 4344050720785) 	γ-Al_2O_3 (20nm) + water	Under turbulent flow, 0.15 vol% γ-Al_2O_3 increased heat transfer coefficient and friction factor by 23 and 25% respectively
Double pipe and plate heat exchangers [117] Double tube heat exchanger Inner tube internal diameter: 12 mm Inner tube external diameter: 14 mm Outer tube internal diameter: 50.8 mm Outer tube external diameter: - Test section length: 70 cm Plate heat exchanger Height: 40 cm Length: 60 cm	Al_2O_3 (20 nm) + EG CuO (20 nm) + EG	Fixing nanoparticle concentration at 1 wt% and temperature at 75°C: Al_2O_3–EG showed 26.2 and 38.3%, CuO–EG showed 37.2 and 49.33%, forced convective heat transfer coefficient enhancement in double pipe and plate heat exchangers respectively
Double pipe U-bend heat exchanger [118] (License Number: 4344051163533) 	Fe_3O_4 (36 nm) + water	At Reynolds number 28970, 0.06 vol% Fe_3O_4 nanofluid contributed 14.7% maximum heat transfer enhancement, 1.092 times friction factor, 1.037 times NTU and 1.024 times effectiveness of heat exchanger when compared to water
Air-cooled heat exchanger [119] (License Number: 4344051381205)	hybrid carbon (20–30 nm) nanofluids	At inlet temperature of 35 °C and flow rate of 2.0 L min^{-1}, 0.02 wt% nanoparticles enhanced heat exchange capacity and system efficiency factor were enhanced about 13.0 and 11.7% respectively. Higher coolant flow rate increased these two parameters also

Table 5 continued

[a]All units in mm

Cone helically coiled tube heat exchanger [120] Coiled angle: 8 degree Internal cone helical coiled tube diameter: 8 mm External diameter of cone helical coiled tube: 10 mm Shell diameter: 114 mm Effective length of the coil: 5000 mm Coil pitch: 20 mm Length of calming section: 110 mm Cone helical coil diameter: 64 mm	MWCNT (50–80 nm) + water	0.1, 0.3 and 0.5 vol% MWCNT raise Nusselt number and pressure drop at tube side for 22, 41, 52 and 25, 50, 81% respectively, under laminar flow of Dean number from 481 to 2130
Counter flow heat exchanger [121] (License Number: 4344060382711)	Ag (30–90 nm) + water/EG (70:30)	At 0.45 vol% Ag, 42% maximum enhancement of convective heat transfer coefficient was obtained. Authors suggested optimum concentration of 0.15 vol% to avoid significant increment of pressure drop
Cross flow heat exchanger [122] (License Number: 4344060520375)	Fe_2O_3 + water and Al_2O_3 + water	0.65 vol% Fe_2O_3 and Al_2O_3 nanofluids showed 9 and 7% of heat transfer enhancement when compared to water
Cross flow heat exchanger [123] Multi-louvered aluminium fins Number of tubes: 38 Number of fins per tube: 70	Al (84 nm) + double-distilled water	0.2 and 0.3 vol% nanofluids increased effectiveness of the heat exchanger by 8.77 and 11.57% respectively. Heat transfer coefficient was increased by 16.40 and 18.39% by dispersing 0.2 and 0.3 vol% Al nanoparticles into water respectively

[a]All nanoparticles diameter shown is mean diameter

nanocoolant. When the Reynolds number of nanocoolant and air was set to 5000 and 6000, respectively, 2 vol% of copper was sufficient to increase heat transfer by 3.8% compared to base fluid. In addition, frontal area of radiator was estimated to have 18.7% of contraction.

Comparison between CuO, Al$_2$O$_3$ and TiO$_2$ water-based nanofluids was made by few researchers. Togun et al. [136] looked up turbulent heat transfer of these three nanofluids in an annular concentric pipe. Firstly, they prepared Al$_2$O$_3$ nanofluid experimentally and validated numerical results from experimental results. $k - \varepsilon$ turbulence model was considered in ANSYS Fluent software. At expansion ratio of 2, heat transfer augmentation and pressure drop for TiO$_2$, CuO and Al$_2$O$_3$ were 45.2, 47.3, 49 and 62.6, 65.4, 57.6%, respectively. Khan and his partner [137] tested all nanofluids; CuO nanofluid exhibited highest heat transfer rate. It was noticed that heat transfer rate was increased with increasing concentration, which is in line with the finding of Ahmad et al. [138] who compared Cu, Al$_2$O$_3$ and SiO$_2$ water-based nanofluids. In this study, the boundary conditions set were consistent heat flux (18,000 W cm^{-2}) and laminar flow (Re = 100–1000).

Hussein et al. [139] considered inlet temperature of 60–90 °C and Reynolds number of 10,000–100,000 in a 500-mm radiator flat tube. The maximal value for Nusselt number and friction factor increment was 18 and 12%, respectively, for 4 vol% TiO$_2$ nanoparticle in water-based nanofluid. Performance of nanocoolant in class 8 truck engine was determined by Saripella et al. [140]. The coolant was made up of CuO and water/ethylene glycol. They observed that low engine and coolant temperature gave high heat transfer coefficient.

Using ANSYS Fluent software, Fsadni et al. [141] investigated thermal and flow performance of Al$_2$O$_3$–water nanofluid in a helically coiled tube heat exchanger with curvature of 0.032–0.052. Single-phase homogeneous model was used to compute the turbulent flow condition with constant heat flux and Reynolds number of 10,000–60,000. Heat transfer performance and pressure drop were increased by 7–34 and 11–63%, respectively, at concentration of 1–4 vol%. Furthermore, increasing curvature ratio could boost extra 2.5 and 4.7% in heat transfer performance and pressure drop.

Other applications

Not only cooling system in vehicle is concerned nowadays, various applications such as solar collector, processors for electronic devices and thermal energy storage unit are dependent on excellent heat transfer fluid to achieve high efficiency with better thermal and flow properties. Until today, the demand of nanofluid in different fields is kept on increasing. A number of papers related to nanofluid in Scopus are shown in Fig. 8. It is clearly shown that the demand on using nanofluid in engineering field is leading among other fields, and thus, it is important to further explore the subtle mechanism of nanofluid enhancing performance in the approach.

Solar thermal collector

Solar thermal collector is used to capture thermal energy emitted from solar radiation, and it is usually called solar energy. Solar energy is one of the most commonly used renewable resources to promote greener environment, and thus, many modifications were done on geometrical part of absorbers in solar collectors to increase thermal efficiency. Anyhow, there is limitation on the optimization method

Fig. 8 Number of published papers related to 'nanofluid' in Scopus till January 2018
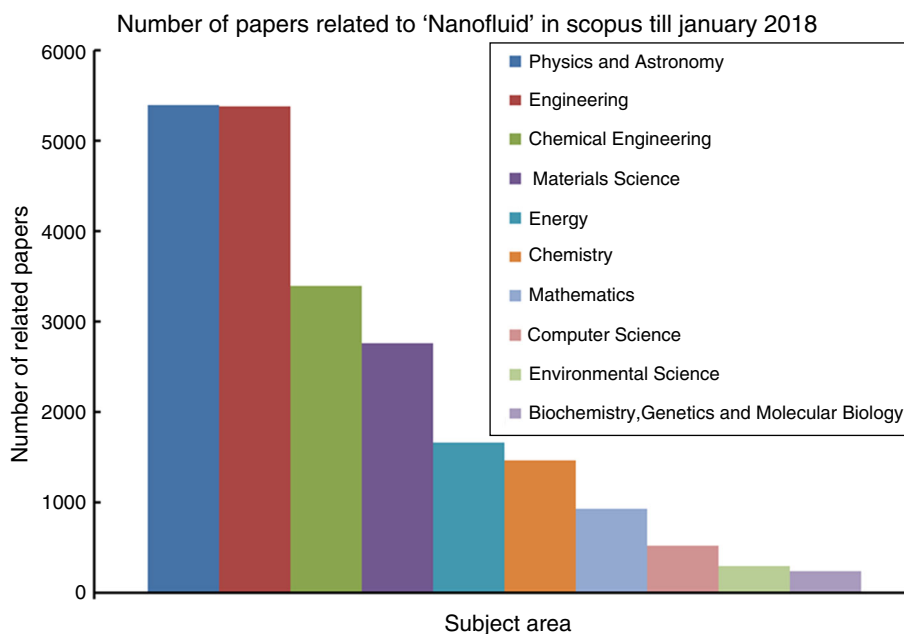
due to significant increment of pressure drop [142]. Thus, excellent heat transfer fluid is vital to ensure further increment of thermal efficiency of solar collectors, whereby nanofluid is used instead of conventional working fluid–water. For instance, increasing concentration of CuO–water nanofluid was reported to give positive impact on thermodynamic efficiency and energy efficiency in a solar-driven combined cooling, heating and power (CCHP) system [143].

Specific heat capacity of salt-based nanofluids was examined by Hu and his co-workers [144]. Firstly, Al_2O_3 nanoparticles with diameter of 20 nm were mixed with water; then, $NaNO_3$ and KNO_3 which are solar salts are added into the suspension. With 2.0% of nanoparticle concentration, the specific heat capacity was enhanced up to 8.3%. They also found that Coulombic energy was the main contributor of the increment of specific heat capacity.

Jin and Jing [145] proposed a novel liquid optical filter for hybrid photovoltaic/thermal (PVT) application. They prepared magnetic electrolyte nanofluids (ENFs) which contained magnetic Fe_3O_4 and water/ethylene glycol. Then, methylene blue and copper sulfate were added separately to produce two different nanofluids, which are denoted as ENF-1 and ENF-2, respectively, in Fig. 9. Their results revealed that both nanofluids have better thermal conductivity than base fluid in tested temperature of 20–60 °C and performed better than conventional core/shell nanoparticle nanofluid filters.

To determine thermal performance, thermal conductivity and viscosity of Ag–water nanofluid, Koca et al. [146] carried out experiment on a single-phase natural convection mini loop. The nanofluid contained 5 mass%, 15 nm and spherical-shaped Ag nanoparticles and 1.25 mass% polyvinylpyrrolidone (PVP) surfactant. In their analysis, they found that the effectiveness of mini loop was enhanced to 11% with 1 mass% of Ag nanoparticle. Besides that, their results obtained were consistent with their previous work which stated that PVP was the barrier on heat transfer performance at ambient temperature. At 23 °C, thermal conductivity of nanofluid decreased for 11.5% when the Ag concentration was 1 mass%, whereas viscosity was increased by 4.81% at 20 °C with the same concentration.

In another experimental study conducted by Tahat and Benim [147], they investigated thermophysical and rheological properties of hybrid nanofluid which contained Al_2O_3 and CuO nanoparticles in flat plate solar collector. Water and ethylene glycol were served as the base fluid in ratio of 25:75 by mass. The volume concentration of nanoparticles was varied from 0.5 to 2, and 45% of enhancement was observed on the efficiency of solar collector.

An experimental study by Manikandan and Rajan [148] involved determination of viscosity and thermal conductivity of sand–propylene glycol–water nanofluid in solar energy collection. 16.3% of thermal conductivity increment and 47% of viscosity decrement were obtained through testing 2 vol% of the nanofluid at 28 °C. They pointed out that the rising of thermal conductivity was caused by Brownian motion, which is in line with the finding from Devireddy et al. [128]. Accordingly, efficiency of solar energy collection was improved by 16.5 and 9% when 2 and 0.5 vol% of the nanofluid were used.

Saidur et al. [149] found out that nanofluid is able to provide superior optical properties and better heat transfer as volumetric absorber in direct solar collector. From their simulation results, alumina–water nanofluid improved the absorption capability at shorter and visible wavelength area

Fig. 9 Thermal conductivities of ENFs and base fluid
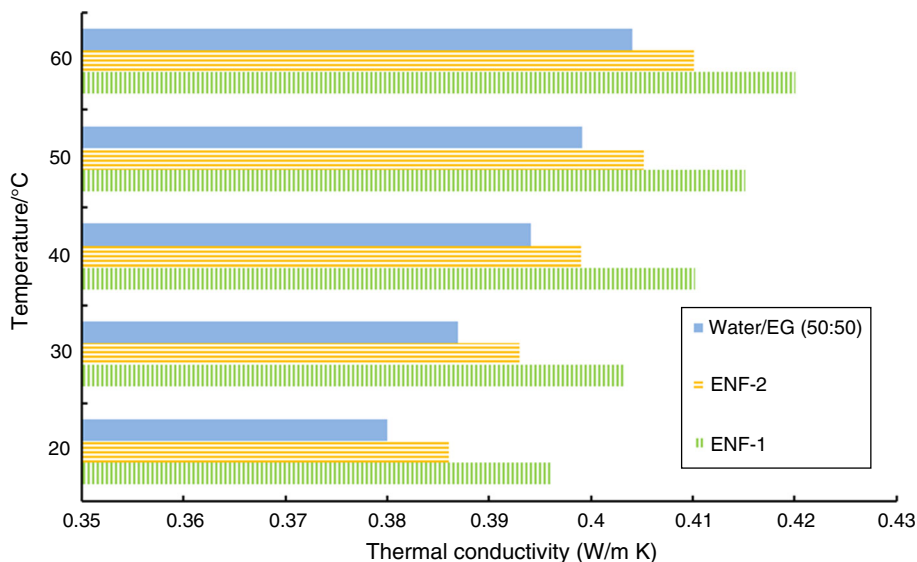
when compared to water. When the amount of Al_2O_3 was raised to 1.0 vol%, the nanofluid was nearly non-transparent to light wave. They also proposed that concentration of nanoparticles has a linear proportional relationship with extinction coefficient.

Bellos and Tzivanidis [150] numerically investigated six different oil-based nanofluids in parabolic trough collectors (PTC). In their analysis, concentration of nanofluids (up to 6%), flow rate (50–300 L min^{-1}), inlet temperature (300–650 K) and solar irradiation level were studied. Their results revealed that nanofluid with Cu nanoparticles exhibits the most thermal efficiency enhancement, while SiO_2 the lowest. Maximum thermal efficiency enhancement of 2.2% was found at 6% Cu concentration, 600 K inlet temperature and flow rate of 50 L min^{-1}. In addition, thermal efficiency enhancement did not show a significant increment when nanoparticles concentration exceed 4%. A new evaluation index that includes heat transfer coefficient, density-specific heat capacity and flow rate was found able to determine thermal efficiency enhancement of PTC.

Another numerical study by Bellos et al. [151] was about two different methods to enhance thermal efficiency of linear Fresnel reflector. The use of finned absorber and CuO–thermal oil nanofluid with three different concentrations (2, 4, 6%) was compared under different inlet temperatures and flow rates. It was found that combination of these two approaches showed the highest thermal efficiency enhancement (0.82%), while adding 4% concentration nanofluid and using finned absorber improved thermal efficiency by 0.28 and 0.61%, respectively. Besides that, peripheral receiver temperature variation was reduced using both methods, and this could lead to slower deformation of the receiver. Although pumping work was increased using these enhancement methods, global performance of the collector was still favorable.

Heat sink in electronics cooling system

In electronics field, passive cooling method is commonly used due to the absence of external parts and low cost. There are some passive techniques which have been employed for heat transfer improvement, such as applying corrugated surfaces, rough surfaces, installing flow swirling tools and using porous materials [152]. However, passive method itself is not sufficient for cooling purpose due to rapid growing of complex systems in electronic devices. From Sidik's review [153] on passive cooling technique for microchannel heat sink, he suggested the implantation of nanofluid may further facilitate cooling performance.

Jang and Choi [154] introduced the combination between nanocoolant and microchannel heat sink in order to provide high cooling performance using active cooling method. They investigated 6-nm Cu nanoparticles and 2-nm diamond nanoparticles, both with 1 vol% concentration dispersed in water under temperature difference of 80 °C between ambient temperature and junction temperature. Cooling performance of the microchannel heat sink was enhanced by 4 and 10% by Cu nanofluid and diamond nanofluid, respectively, due to lower thermal resistance of these nanofluids compared to water as shown in Fig. 10.

Forced convective heat transfer of CuO/water nanofluid in microchannel heat sink was studied by Chabi and his co-workers [155]. At channel entrance region with Reynolds number of 1150, the average heat transfer coefficient of 0.2 vol% nanofluid was 40% higher compared to deionized water. However, they noticed heat transfer deterioration when Reynolds number was further increased. Recent work from Sun and Liu [156] showed the heat transfer coefficient of Al_2O_3 nanofluid and CuO nanofluid in a liquid-cooled central processing unit (CPU) radiator. 0.1–0.5 mass% nanoparticles and Reynolds number of 400–2000 were varied. Convective heat transfer coefficient of Al_2O_3 nanofluid and CuO nanofluid was about 1.1–1.6 times and 1.1–2 times higher than that of deionized water.

A major study on heat transfer performance of ERG aluminum foam heat sink in a computer processor (Intel core i7) was carried out experimentally and numerically by Bayomy and Saghir [157]. They produced γ-Al_2O_3/water nanofluid with volume concentration of 0.1–0.6% and tested in laminar flow (Reynolds number of 210–631) and heat flux of 8.5–13.8 W cm^{-2}. Their results showed that 0.2 vol% nanofluid yielded the highest local Nusselt number. For average Nusselt number, 37 and 28% of enhancement for 0.2 vol% nanofluid over pure water were seen at Reynolds number of 601.3 and 201, respectively. In addition to that, the numerical results obtained showed low discrepancies up to 3 and 2% for local Nusselt number and local temperature, respectively.

Arjun and Rakesh [158] determined the thermal and flow performance of 23 nm Al_2O_3–water nanofluid in circular microchannel numerically. Reynolds number of 5–11,980 and 0–5 vol% of Al_2O_3 generated heat transfer enhancement of 83%. Convective heat transfer of Al_2O_3 in square microchannel under laminar flow was studied by Irwansyah et al. [159] experimentally. 0.6 and 1.0 vol% water-based alumina nanofluids showed enhancement of 6.9 and 21%, respectively. Effect of three different microchannel shapes was numerically investigated by Toghraie et al. [160]. Their results revealed that sinusoidal microchannel without nanofluid showed higher heat transfer rate than smooth microchannel with nanofluid. Among all shapes, zigzag microchannel is suggested as the best microchannel.

**Fig. 10** Numerical result obtained at pumping power up to 2.50 kW
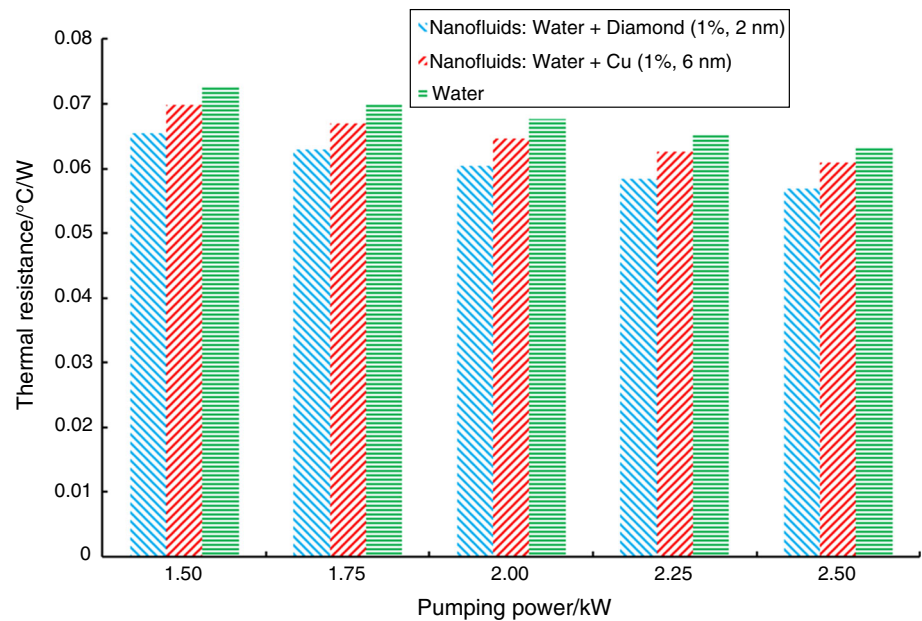
Flow boiling

Boiling is a technique using latent heat transport to increase heat transfer performance in industrial applications such as power plants, electronics cooling system, heat pipes and nuclear reactors [161]. Flow boiling is one of the common mechanisms used in thermal engineering applications. Due to the growing demand from those huge applications, nanofluid has been used to replace or enhance the properties of conventional heat transfer fluid.

Zangeneh et al. [162] reported the effects of nanoparticles synthesis method and subcooled flow boiling on heat transfer performance in a vertical annulus. They observed that ZnO which modified by using amine and UV irradiation gave the highest heat transfer performance (8.14%) compared to water. In addition to that, shape of nanoparticles plays a vital role in heat transfer coefficient as nanotube–nanorod shape performed better than spherical shape.

Refrigerant (R113) mixed with CuO was tested in a smooth copper tube with 150 cm length, 0.07 cm thickness and 0.952 cm outer diameter. 29.7% of maximum intensification in heat transfer coefficient was observed when concentration of CuO was varied in the range of 0–0.5 mass%. The horizontal tube with flow boiling using heating tapes set up by Peng and his team [163] is shown below (Fig. 11).

Researchers from Korea [164] investigated flow boiling experiment using 0.01 vol% alumina–water nanofluid in a horizontal rectangular channel. A disk-shaped copper surface was placed below the rectangular channel to perform flow boiling. At 1 and 4 m s^{-1} nanofluid flow velocity,
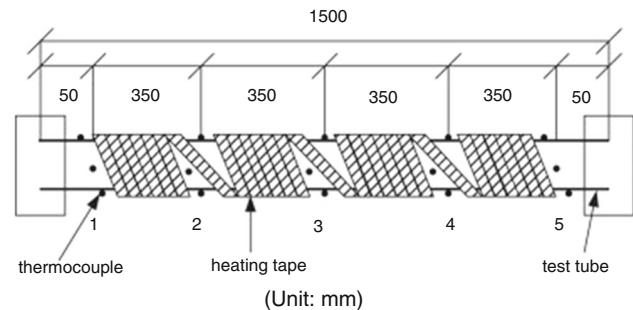
Fig. 11 Test section where flow boiling takes place [163] (License Number: 4347970093882)

critical heat flux (CHF) was increased by 24 and 40%, respectively, when compared to water. The increment in CHF was explained in such way that deposition of nanoparticles caused changes in surface wettability. Same conclusion was obtained by Vafaei and Wen [165] who inspected the effect of subcooled flow boiling on critical heat flux in a horizontal 510-μm microchannel. Under mass flow rate of 600–1650 kg m^{-3}, 0.1 vol% alumina-deionized water nanofluid remarkably increased CHF for 51%. Another study showed that 0.005 vol% MWCNT nanofluid enhanced heat transfer coefficient of pure water by 4.3% at CHF [166].

Investigation into the flow boiling heat transfer behavior of evaporator vertical surface in a thermosyphon loop was carried out by Yang and Liu [167]. Average 50 nm CuO nanoparticles were suspended into water, and different mass concentrations of nanofluid were prepared (0.1–1.5 mass%). Maximum value of heat transfer coefficient was found at optimal 1.0 mass% CuO, whereas 29% of increment in CHF was observed at 1.5 mass% CuO.
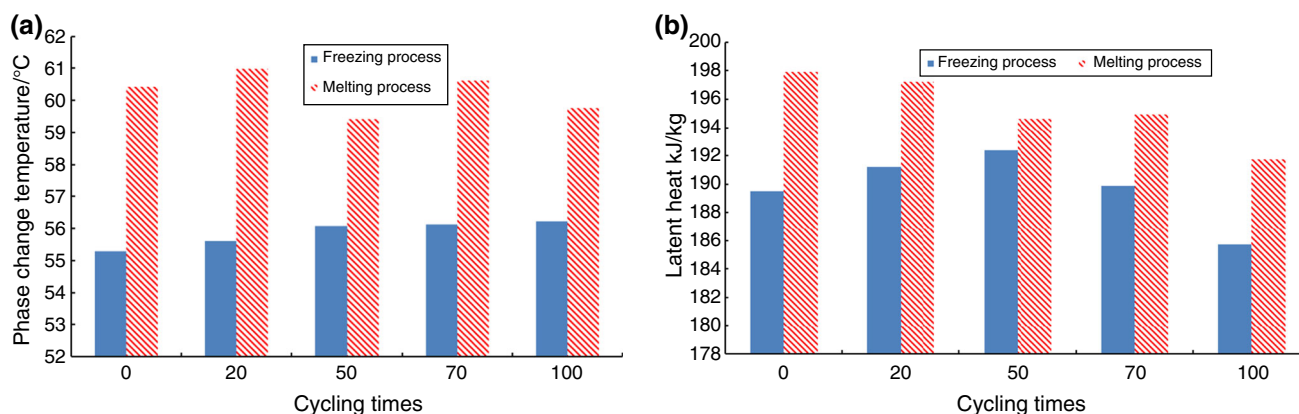
Fig. 12 Effect of thermal cycles on **a** phase change temperature and **b** latent heat of the PCM

Thermal energy storage system with phase change material

Thermal energy storage system (TESS) functions to store and release energy in the form of latent heat and sensible heat for consequent uses to conserve waste heat from surrounding. Phase change material is commonly used in thermal energy storage system (TESS) due to their excellent capability to store and release energy during density changes. Thus, the criteria for enhanced heat transfer performance in TESS are mainly melting duration, melting temperature and latent heat of fusion of phase change material (PCM).

Behavior of alumina–water nanofluid in TTES was initially studied by Wu et al. [168] experimentally. They found out that 0.2 mass% alumina in water reduced supercooling temperature by 70.9% and total freezing time by 20.5%. In addition, thermal conductivity was enhanced by 10.5%. Years later, Wu and his team [169] made comparison between behavior of Cu, Al and C/Cu nanoparticles when each of them was dispersed into melting paraffin. Best transfer performance was observed when 0.5 mass% Cu nanoparticles were used. Also, latent heat for freezing and melting was reduced by 11.7 and 11.1%, respectively. Figure 12 shows 1 mass% Cu/paraffin PCM with excellent thermal reliability even after 100 cycles of cooling and heating.

Behavior of nanofluids in an unit of upright shell-and-tube TESS was explored by Duan and his partner [170]. They established a computational fluids dynamics model to carry out their numerical study. As novelty in their study, CuO–water nanofluid acted as heat transfer fluid (HTF) and CuO–paraffin nanoparticle-enhanced phase change material (NePCM) was used on shell side of the energy storage unit. Nanoparticle size considered was 10 nm in diameter, and concentration range for HTF and NePCM was 0–7 and 0–4 vol%, respectively. From their analysis, inclusion of nanoparticles not only improved heat transfer coefficient but accelerated melting process of PCM. However, exceeding amount of nanoparticles in PCM could lead to heat transfer and melting rate degradation as viscosity would be increased gradually. Using response surface methodology (RSM), it was found that inlet temperature of HTF was the most compelling parameter compared to concentration of HFT and NePCM.

Sebti et al. [171] carried out numerical investigation on the effect of CuO–NePCM on heat transfer performance in a horizontal annulus with concentric cylindrical shape. 0–0.05 vol% CuO and 5–20 °C temperature difference were their manipulating parameters. Their results showed that higher concentration of CuO reduced solidification time and heat transfer rate was increased.

Tasnim and his team [172] demonstrated scale analysis and numerical study on phase change process of NePCM in a porous-latent HTES. Initially, the extent of entire phase change process was appraised using scale analysis. The analysis provided relationship between various parameters (Rayleigh number, Stefan number, Nusselt number, Fourier number, nanoparticle concentration and porosity of the porous medium). Then, Darcy model was used to solve the melting phenomenon of NePCM in a rectangular enclosure with porous medium under natural convection condition. Exceptionally, both scale analysis and numerical study revealed that the existence of NePCM corrupted the convection and conduction heat transfer performance in the enclosure. Moreover, the melting time of NePCM was longer than PCM.

Conclusions

This paper presents recent review on the effects of implantation of nanofluid in vehicle engine cooling system and other major applications. Based on studies, it is found that nanoparticles can be used to enhance thermophysical properties of working fluid, especially thermal

conductivity. Improved thermal conductivity of nanofluid is due to the higher thermal properties of dispersed solid nanoparticles, and this leads to:

1. Increased cooling performance/overall system efficiency. Higher thermal conductivity means better capability of a substance to absorb and release heat efficiently. This results in more heat which can be dissipated away from a system.
2. Reduced system size. When a more efficient working fluid is used, increment of surface area of heat exchanger or pipe by adding fins or modifying geometric is not needed. This can also help to reduce the drag on car which reduce fuel consumption.
3. Reduced storage of heat transfer fluid. Conventional coolants need larger storage volume so that the cooling system does not get overheated easily when heated coolant keep flowing back into storage tank. Nanofluids with better cooling rate require less volume than conventional fluid.
4. Strengthen system lifespan. Overheating would result in mechanical failure. Thus, nanofluids with better cooling performance can help to protect body of heat exchanger and cooling system.
5. Reduced pumping power when compared to same amount of heat transfer from conventional fluid. When nanofluids are used, both heat transfer rate and pressure drop will increase. As reported by past researchers, heat transfer rate increment is much more significant when compared to pressure drop. Thus, when amount of heat transfer is the same for both conventional coolant and nanofluid, nanofluid is believed to show less pressure drop.

For all of its aforementioned advantages, nanofluid in fact is something of a double-edged sword. Although increasing concentration of nanoparticles can greatly enhance heat transfer performance of cooling system, excessive amount of nanoparticles will lead to high viscosity of nanofluids which contributes to increment of pressure drop and may be followed by deterioration of overall efficiency of a particular system due to clogging and agglomeration of nanoparticles. However, this can be overcome by increasing working temperature which reduces viscosity of nanofluids and in the same time increases thermal conductivity. It has to be noted that extremely high working temperature can lead to mechanical system breakdown.

In short, nanofluids can be a promising working fluid for various cooling systems due to its superior heat transfer performance. Overall, effective and efficiency of a system can be improved when conventional working fluid is replaced by nanofluids.

Current challenges and recommendation

From authors' review, most of the results are in positive favor in which nanoparticles enhance cooling capability or heat transfer performance of conventional heat transfer fluid in various heat transfer applications. For cases where heat transfer deterioration occurred, few researchers reported that excessive amount of nanoparticles is the factor where agglomeration happens. Among them, very few mentioned on the optimum amount of nanoparticles before deterioration of performance or thermal properties would occur. Consequently, repeating experimental work in the future on the same nanoparticles and similar working parameters is needed to obtain the optimum concentration. Knowing the optimum amount of nanoparticles can obtain the best thermal performance for a system.

Secondly, there are many past researchers that could not reach consensus on the exact factors which affect heat transfer behavior of nanofluid. This may due to different variables used in their respective experiment or numerical study such as working temperature and system pressure. In addition, the challenging part is to produce desirable nanofluids and compare to each other. Some researchers compared the heat transfer enhancement of different nanoparticles by omitting these few aspects:

1. Huge difference of mean diameter size. Few past studies showed that smaller size of nanoparticles has better thermal performance due to increased surface area over volume ratio. Anyhow, many researchers are comparing different nanofluids with different nanoparticles sizes. It is inaccurate to judge performance of particular nanoparticles under such circumstances.
2. Shape of nanoparticles. From review, thermal performance results from different nanoparticles shapes are quite significant as shown by Hatami et al. [133]. Most researchers carried out the comparison on the performance between different nanofluids with different nanoparticles shapes, which caused lack of agreement in their results.
3. Degree of stability. Many past researchers used two-step method to prepare nanofluids. Some of them used sedimentation method to observe the presence of sediments of nanofluids after certain period. Then, nanofluids are considered stable when no sediments are observed. The actual degree of stability is unknown. There is a lack of measurement standard on the stability of nanofluids. Although there are many other inspection methods such as spectral absorbance analysis, zeta potential measurement and pH value adjustment, these methods are not chosen due to either high cost or more steps. Stability of nanofluids should be

evaluated using same method before any comparison work is performed.

For future work, main factors affecting thermal conductivity need to be identified. It is important to understand the mechanism which thermal conductivity is greatly affected. The three aspects mentioned above are believed to contribute the most to the magnitude of thermal conductivity of nanofluids. In order to determine impact of each parameter, it is vital to control only one of the variables in experiment. By this way, the main parameter which gives the highest impact to thermal conductivity can be determined more accurately.

In addition, heat transfer performance as a function of parameters such as temperature, pressure and flow rate can be developed as correlation, and impact of each parameter can be determined. To obtain results which are more accurate and reliable, more experimental works have to be carried out systematically. Also, a generalized equation for each type of nanoparticles can be developed. More experimental works using the same preparation method, stability evaluation analysis and physical properties of nanoparticles are needed so that more accurate data are available to develop such equation. This can help future researchers to study behavior of nanoparticles more easily and in the same time provides industry reliable data to commercialize nanofluids into more applications.

Major problems with the inclusion of nanofluids into daily applications are the stability and price of nanofluids. Therefore, more works are needed to improve these drawbacks to implement nanotechnology in this century. In short, current investigation works on nanofluid need to be improved from several aspects and at the same time improve current theoretical model so that feasible use of nanofluids in future researches and industries can be complied.

References

1. Choi SU, Eastman JA. Enhancing thermal conductivity of fluids with nanoparticles. Lemont: Argonne National Lab.; 1995.
2. Wen D, Lin G, Vafaei S, Zhang K. Review of nanofluids for heat transfer applications. Particuology. 2009;7(2):141–50.
3. Aravind SSJ, Ramaprabhu S. Graphene-multiwalled carbon nanotube-based nanofluids for improved heat dissipation. RSC Adv. 2013;3(13):4199–206.
4. Liu MS, Lin MC, Huang IT, Wang CC. Enhancement of thermal conductivity with CuO for nanofluids. Chemical engineering & technology. 2006;29(1):72–7.
5. Yu W, Xie H, Chen L, Li Y. Investigation of thermal conductivity and viscosity of ethylene glycol based ZnO nanofluid. Thermochim Acta. 2009;491(1):92–6.
6. Selvam C, Solaimalai Raja R, Mohan Lal D, Harish S. Overall heat transfer coefficient improvement of an automobile radiator with graphene based suspensions. Int J Heat Mass Transf. 2017;115:580–8.
7. Islam R, Shabani B, Andrews J, Rosengarten G. Experimental investigation of using ZnO nanofluids as coolants in a PEM fuel cell. Int J Hydrog Energy. 2017;42(30):19272–86.
8. Azmi WH, Abdul Hamid K, Mamat R, Sharma KV, Mohamad MS. Effects of working temperature on thermo-physical properties and forced convection heat transfer of TiO_2 nanofluids in water–ethylene glycol mixture. Appl Therm Eng. 2016;106:1190–9.
9. Mugilan T, Sidik NAC, Japar W. The use of smart material of nanofluid for heat transfer enhancement in microtube with helically spiral rib and groove. J Adv Res Mater Sci. 2017;32(1):1–12.
10. Abubakar S, Sidik NC. Numerical prediction of laminar nanofluid flow in rectangular microchannel heat sink. J Adv Res Fluid Mech Therm Sci. 2015;7(1):29–38.
11. Che Sidik NA, Witri Mohd Yazid MNA, Mamat R. Recent advancement of nanofluids in engine cooling system. Renew Sustain Energy Rev. 2017;75(Supplement C):137–44.
12. Lee S, Choi S-S, Li S, Eastman J. Measuring thermal conductivity of fluids containing oxide nanoparticles. J Heat Transf. 1999;121(2):280–9.
13. Kole M, Dey T. Viscosity of alumina nanoparticles dispersed in car engine coolant. Exp Therm Fluid Sci. 2010;34(6):677–83.
14. Namburu PK, Kulkarni DP, Misra D, Das DK. Viscosity of copper oxide nanoparticles dispersed in ethylene glycol and water mixture. Exp Therm Fluid Sci. 2007;32(2):397–402.
15. Wang X, Xu X, Choi SUS. Thermal conductivity of nanoparticle–fluid mixture. J Thermophys Heat Transf. 1999;13(4):474–80.
16. Das SK, Putra N, Thiesen P, Roetzel W. Temperature dependence of thermal conductivity enhancement for nanofluids. J Heat Transf. 2003;125(4):567–74.
17. Chen J, Jia J. Experimental study of TiO_2 nanofluid coolant for automobile cooling applications. Mater Res Innov. 2017;21(3):177–81.
18. Elias M, Mahbubul I, Saidur R, Sohel M, Shahrul I, Khaleduzzaman S, et al. Experimental investigation on the thermophysical properties of Al_2O_3 nanoparticles suspended in car radiator coolant. Int Commun Heat Mass Transf. 2014;54:48–53.
19. Arzani HK, Amiri A, Arzani HK, Rozali SB, Kazi S, Badarudin A. Toward improved heat transfer performance of annular heat exchangers with water/ethylene glycol-based nanofluids containing graphene nanoplatelets. J Therm Anal Calorim. 2016;126(3):1427–36.
20. Selvam C, Lal DM, Harish S. Thermal conductivity and specific heat capacity of water–ethylene glycol mixture-based nanofluids with graphene nanoplatelets. J Therm Anal Calorim. 2017;129(2):947–55.
21. Garbadeen I, Sharifpur M, Slabber J, Meyer J. Experimental study on natural convection of MWCNT–water nanofluids in a square enclosure. Int Commun Heat Mass Transf. 2017;88:1–8.
22. Thakur M, Gangacharyulu D, Singh G. Effect of temperature and multiwalled carbon nanotubes concentration on thermophysical properties of water base nanofluid. IJE Trans. B Appl. 2017;30(8):1223–30.
23. Ilyas SU, Pendyala R, Narahari M. Stability and thermal analysis of MWCNT-thermal oil-based nanofluids. Colloids Surf A. 2017;527(Supplement C):11–22.
24. Amiri M, Movahedirad S, Manteghi F. Thermal conductivity of water and ethylene glycol nanofluids containing new modified surface SiO_2–Cu nanoparticles: experimental and modeling. Appl Therm Eng. 2016;108:48–53.

25. Abdolbaqi MK, Sidik NAC, Rahim MFA, Mamat R, Azmi W, Yazid MNAWM, et al. Experimental investigation and development of new correlation for thermal conductivity and viscosity of BioGlycol/water based SiO_2 nanofluids. Int Commun Heat Mass Transf. 2016;77:54–63.

26. Chiam H, Azmi W, Usri N, Mamat R, Adam N. Thermal conductivity and viscosity of Al_2O_3 nanofluids for different based ratio of water and ethylene glycol mixture. Exp Therm Fluid Sci. 2017;81:420–9.

27. Sundari KG, Asirvatham LG, Kumar TMN, Ahammed N. Measurement of thermophysical properties of Al_2O_3/glycerin (G13) nanofluid for automotive radiator cooling applications. Res J Chem Environ. 2017;21(3):17–24.

28. Nabil M, Azmi W, Hamid KA, Mamat R, Hagos FY. An experimental study on the thermal conductivity and dynamic viscosity of TiO_2–SiO_2 nanofluids in water: ethylene glycol mixture. Int Commun Heat Mass Transf. 2017;86:181–9.

29. Adhami Dehkordi R, Hemmat Esfe M, Afrand M. Effects of functionalized single walled carbon nanotubes on thermal performance of antifreeze: an experimental study on thermal conductivity. Appl Therm Eng. 2017;120(Supplement C):358–66.

30. Iqbal SM, Raj CS, Michael JJ, Irfan AM. A comparative investigation of Al_2O_3/H_2O, SiO_2/H_2O and ZrO_2/H_2O nanofluid for heat transfer applications. Dig J Nanomater Biostruct. 2017;12(2):255–63.

31. Chen L, Cheng M, Yang D, Yang L. Enhanced thermal conductivity of nanofluid by synergistic effect of multi-walled carbon nanotubes and Fe_2O_3 nanoparticles. Appl Mech Mater. 2014;548–549:118–123.

32. Murshed SMS, Leong KC, Yang C. Enhanced thermal conductivity of TiO_2–water based nanofluids. Int J Therm Sci. 2005;44(4):367–73.

33. Assael MJ, Chen C-F, Metaxa I, Wakeham WA. Thermal conductivity of suspensions of carbon nanotubes in water. Int J Thermophys. 2004;25(4):971–85.

34. Xuan Y, Li Q. Heat transfer enhancement of nanofluids. Int J Heat Fluid Flow. 2000;21(1):58–64.

35. Hong T-K, Yang H-S, Choi C. Study of the enhanced thermal conductivity of Fe nanofluids. J Appl Phys. 2005;97(6):064311.

36. Chen H, Yang W, He Y, Ding Y, Zhang L, Tan C, et al. Heat transfer and flow behaviour of aqueous suspensions of titanate nanotubes (nanofluids). Powder Technol. 2008;183(1):63–72.

37. Chougule SS, Sahu SK. Comparative study of cooling performance of automobile radiator using Al_2O_3–water and carbon nanotube-water nanofluid. J Nanotechnol Eng Med. 2014;5(1):010901–6.

38. Li X, Zou C, Qi A. Experimental study on the thermo-physical properties of car engine coolant (water/ethylene glycol mixture type) based SiC nanofluids. Int Commun Heat Mass Transf. 2016;77:159–64.

39. Hemmat Esfe M, Saedodin S. Turbulent forced convection heat transfer and thermophysical properties of Mgo–water nanofluid with consideration of different nanoparticles diameter, an empirical study. J Therm Anal Calorim. 2015;119(2):1205–13.

40. Afshari A, Akbari M, Toghraie D, Yazdi ME. Experimental investigation of rheological behavior of the hybrid nanofluid of MWCNT–alumina/water (80%)–ethylene-glycol (20%). J Therm Anal Calorim. 2018;132(2):1001–15.

41. Ahammed N, Asirvatham LG, Wongwises S. Effect of volume concentration and temperature on viscosity and surface tension of graphene–water nanofluid for heat transfer applications. J Therm Anal Calorim. 2016;123(2):1399–409.

42. Maxwell JC. A treatise on electricity and magnetism. Wotton-under-Edge: Clarendon press; 1881.

43. Hamilton R, Crosser O. Thermal conductivity of heterogeneous two-component systems. Ind Eng Chem Fundam. 1962;1(3):187–91.

44. Yu W, Choi SUS. The role of interfacial layers in the enhanced thermal conductivity of nanofluids: a renovated Maxwell model. J Nanopart Res. 2003;5(1–2):167–71.

45. Koo J, Kleinstreuer C. Erratum: a new thermal conductivity model for nanofluids (Journal of Nanoparticle Research (2004) 6 (577–588)). J Nanopart Res. 2005;7(2–3):324.

46. Pak BC, Cho YI. Hydrodynamic and heat transfer study of dispersed fluids with submicron metallic oxide particles. Exp Heat Transf Int J. 1998;11(2):151–70.

47. Maïga SEB, Palm SJ, Nguyen CT, Roy G, Galanis N. Heat transfer enhancement by using nanofluids in forced convection flows. Int J Heat Fluid Flow. 2005;26(4):530–46.

48. Corcione M. Empirical correlating equations for predicting the effective thermal conductivity and dynamic viscosity of nanofluids. Energy Convers Manag. 2011;52(1):789–93.

49. Einstein A. A new determination of molecular dimensions. Ann Phys. 1906;19:289–306.

50. Batchelor GK. The effect of Brownian motion on the bulk stress in a suspension of spherical particles. J Fluid Mech. 1977;83(1):97–117.

51. Gherasim I, Roy G, Nguyen CT, Vo-Ngoc D. Experimental investigation of nanofluids in confined laminar radial flows. Int J Therm Sci. 2009;48(8):1486–93.

52. Tiwari RK, Das MK. Heat transfer augmentation in a two-sided lid-driven differentially heated square cavity utilizing nanofluids. Int J Heat Mass Transf. 2007;50(9):2002–18.

53. Khanafer K, Vafai K. A critical synthesis of thermophysical characteristics of nanofluids. Int J Heat Mass Transf. 2011;54(19):4410–28.

54. Ho CJ, Liu WK, Chang YS, Lin CC. Natural convection heat transfer of alumina–water nanofluid in vertical square enclosures: an experimental study. Int J Therm Sci. 2010;49(8):1345–53.

55. Mintsa HA, Roy G, Nguyen CT, Doucet D. New temperature dependent thermal conductivity data for water-based nanofluids. Int J Therm Sci. 2009;48(2):363–71.

56. Chon CH, Kihm KD, Lee SP, Choi SUS. Empirical correlation finding the role of temperature and particle size for nanofluid (Al_2O_3) thermal conductivity enhancement. Appl Phys Lett. 2005;85:153107–10.

57. Nguyen CT, Desgranges F, Roy G, Galanis N, Maré T, Boucher S, et al. Temperature and particle-size dependent viscosity data for water-based nanofluids—hysteresis phenomenon. Int J Heat Fluid Flow. 2007;28(6):1492–506.

58. Putra N, Roetzel W, Das SK. Natural convection of nano-fluids. Heat Mass Transf Waerme- und Stoffuebertragung. 2003;39(8–9):775–84.

59. Anoop K, Kabelac S, Sundararajan T, Das SK. Rheological and flow characteristics of nanofluids: influence of electroviscous effects and particle agglomeration. J Appl Phys. 2009;106(3):034909.

60. Öğüt EB, Kahveci K. Mixed convection heat transfer of ethylene glycol and water mixture based Al_2O_3 nanofluids: effect of thermal conductivity models. J Mol Liq. 2016;224:338–45.

61. Ghanbarpour M, Haghigi EB, Khodabandeh R. Thermal properties and rheological behavior of water based Al_2O_3 nanofluid as a heat transfer fluid. Exp Therm Fluid Sci. 2014;53:227–35.

62. Timofeeva EV, Gavrilov AN, McCloskey JM, Tolmachev YV, Sprunt S, Lopatina LM, et al. Thermal conductivity and particle agglomeration in alumina nanofluids: experiment and theory. Phys Rev E. 2007;76(6):061203.

63. Alawi OA, Sidik NAC, Xian HW, Kean TH, Kazi SN. Thermal conductivity and viscosity models of metallic oxides nanofluids. Int J Heat Mass Transf. 2018;116(Supplement C):1314–25.

64. Shamaeil M, Firouzi M, Fakhar A. The effects of temperature and volume fraction on the thermal conductivity of functionalized DWCNTs/ethylene glycol nanofluid. J Therm Anal Calorim. 2016;126(3):1455–62.

65. Eastman JA, Phillpot SR, Choi SUS, Keblinski P. Thermal transport in nanofluids. Annu Rev Mater Res. 2004;34:219–46.

66. Patel HE, Sundararajan T, Pradeep T, Dasgupta A, Dasgupta N, Das SK. A micro-convection model for thermal conductivity of nanofluids. Pramana J Phys. 2005;65(5):863–9.

67. Charunyakorn P, Sengupta S, Roy SK. Forced convection heat transfer in microencapsulated phase change material slurries: flow in circular ducts. Int J Heat Mass Transf. 1991;34(3):819–33.

68. Chon CH, Kihm KD, Lee SP, Choi SUS. Empirical correlation finding the role of temperature and particle size for nanofluid (Al$_2$O$_3$) thermal conductivity enhancement. Appl Phys Lett. 2005;87(15):1–3.

69. Wasp EJ, Kenny JP, Gandhi RL. Solid–liquid flow: slurry pipeline transportation [pumps, valves, mechanical equipment, economics]. Ser Bulk Mater Handl (United States). 1977;1(4).

70. Takabi B, Salehi S. Augmentation of the heat transfer performance of a sinusoidal corrugated enclosure by employing hybrid nanofluid. Adv Mech Eng. 2014;6:147059.

71. Sarbolookzadeh Harandi S, Karimipour A, Afrand M, Akbari M, D'Orazio A. An experimental study on thermal conductivity of F-MWCNTs–Fe$_3$O$_4$/EG hybrid nanofluid: effects of temperature and concentration. Int Commun Heat Mass Transf. 2016;76:171–7.

72. Afrand M. Experimental study on thermal conductivity of ethylene glycol containing hybrid nano-additives and development of a new correlation. Appl Therm Eng. 2017;110:1111–9.

73. Brinkman H. The viscosity of concentrated suspensions and solutions. J Chem Phys. 1952;20(4):571.

74. de Bruijn H. The viscosity of suspensions of spherical particles (the fundamental η-c and φ relations). Recueil des Travaux Chimiques des Pays - Bas. 1942;61(12):863–74.

75. Mooney M. The viscosity of a concentrated suspension of spherical particles. J Colloid Sci. 1951;6(2):162–70.

76. Nielsen LE. Generalized equation for the elastic moduli of composite materials. J Appl Phys. 1970;41(11):4626–7.

77. Soltani O, Akbari M. Effects of temperature and particles concentration on the dynamic viscosity of MgO–MWCNT/ethylene glycol hybrid nanofluid: experimental study. Physica E. 2016;84:564–70.

78. Asadi A, Asadi M, Rezaei M, Siahmargoi M, Asadi F. The effect of temperature and solid concentration on dynamic viscosity of MWCNT/MgO (20–80)–SAE50 hybrid nano-lubricant and proposing a new correlation: an experimental study. Int Commun Heat Mass Transf. 2016;78:48–53.

79. Rostamian SH, Biglari M, Saedodin S, Esfe MH. An inspection of thermal conductivity of CuO-SWCNTs hybrid nanofluid versus temperature and concentration using experimental data, ANN modeling and new correlation. J Mol Liq. 2017;231:364–9.

80. Esfe MH, Esfandeh S, Saedodin S, Rostamian H. Experimental evaluation, sensitivity analyzation and ANN modeling of thermal conductivity of ZnO–MWCNT/EG–water hybrid nanofluid for engineering applications. Appl Therm Eng. 2017;125:673–85.

81. Zhao N, Li Z. Experiment and artificial neural network prediction of thermal conductivity and viscosity for alumina–water nanofluids. Materials. 2017;10(5):552.

82. Esfe MH, Saedodin S, Sina N, Afrand M, Rostami S. Designing an artificial neural network to predict thermal conductivity and dynamic viscosity of ferromagnetic nanofluid. Int Commun Heat Mass Transf. 2015;68:50–7.

83. Zawrah MF, Khattab RM, Girgis LG, El Daidamony H, Abdel Aziz RE. Stability and electrical conductivity of water-base Al$_2$O$_3$ nanofluids for different applications. HBRC J. 2016;12(3):227–34.

84. Saidur R, Leong KY, Mohammad HA. A review on applications and challenges of nanofluids. Renew Sustain Energy Rev. 2011;15(3):1646–68.

85. Choi S, Yu W, Hull JR, Zhang Z, Lockwood F. Nanofluids for vehicle thermal management: SAE Technical Paper 2001. Report No.: 0148-7191.

86. Selvam C, Lal DM, Harish S. Enhanced heat transfer performance of an automobile radiator with graphene based suspensions. Appl Therm Eng. 2017;123:50–60.

87. Azmi W, Hamid KA, Usri N, Mamat R, Mohamad M. Heat transfer and friction factor of water and ethylene glycol mixture based TiO$_2$ and Al$_2$O$_3$ nanofluids under turbulent flow. Int Commun Heat Mass Transf. 2016;76:24–32.

88. Alosious S, Sarath S, Nair AR, Krishnakumar K. Experimental and numerical study on heat transfer enhancement of flat tube radiator using Al$_2$O$_3$ and CuO nanofluids. Heat Mass Transf. 2017;53(12):3545–63.

89. Goudarzi K, Jamali H. Heat transfer enhancement of Al$_2$O$_3$–EG nanofluid in a car radiator with wire coil inserts. Appl Therm Eng. 2017;118:510–7.

90. Senthilraja S, Vijayakumar K, Gangadevi R. Effects of specific fuel consumption and exhaust emissions of four stroke diesel engine with CuO/water nanofluid as coolant. Arch Mech Eng. 2017;64(1):111–21.

91. Muruganandam M, Kumar P. Experimental analysis of four stroke diesel engine by using carbon nano tubes based nano fluids as a coolant. J Appl Fluid Mech. 2017;10:1–5.

92. Oliveira GA, Contreras EMC, Bandarra Filho EP. Experimental study on the heat transfer of MWCNT/water nanofluid flowing in a car radiator. Appl Therm Eng. 2017;111:1450–6.

93. Gulhane A, Chincholkar S. Experimental investigation of convective heat transfer coefficient of Al$_2$O$_3$/water nanofluid at lower concentrations in a car radiator. Heat Transf Asian Res. 2017;46:1119–29.

94. Sheikhzadeh G, Fakhari M, Khorasanizadeh H. Experimental investigation of laminar convection heat transfer of Al$_2$O$_3$–ethylene glycol–water nanofluid as a coolant in a car radiator. J Appl Fluid Mech. 2017;10(1):209–19.

95. Jagadishwar K, Sudhakar Babu S. Performance investigation of water and propylene glycol mixture based nano-fluids on automotive radiator for enhancement of heat transfer. Int J Mech Eng Technol. 2017;8(7):822–33.

96. Kumar Sai Tejes P, Appalanaidu Y. Experimental investigation of convective heat transfer augmentation using ZnO-proplyene glycol nanofluids in a automobile radiator. Int J Mech Eng Technol. 2017;8(7):1132–43.

97. Moghaieb HS, Abdel-Hamid HM, Shedid MH, Helali AB. Engine cooling using Al$_2$O$_3$/water nanofluids. Appl Therm Eng. 2017;115(Supplement C):152–9.

98. Abdolbaqi MK, Mamat R, Sidik NAC, Azmi WH, Selvakumar P. Experimental investigation and development of new correlations for heat transfer enhancement and friction factor of BioGlycol/water based TiO$_2$ nanofluids in flat tubes. Int J Heat Mass Transf. 2017;108(Part A):1026–35.

99. Sajedi R, Jafari M, Taghilou M. An experimental study on the effect of conflict measurement criteria for heat transfer enhancement in nanofluidics. Powder Technol. 2016;297:448–56.

100. Azmi W, Usri N, Mamat R, Sharma K, Noor M. Force convection heat transfer of Al_2O_3 nanofluids for different based ratio of water: ethylene glycol mixture. Appl Therm Eng. 2017;112:707–19.

101. Yu W, Xie H, Li Y, Chen L, Wang Q. Experimental investigation on the heat transfer properties of Al_2O_3 nanofluids using the mixture of ethylene glycol and water as base fluid. Powder Technol. 2012;230:14–9.

102. Naraki M, Peyghambarzadeh SM, Hashemabadi SH, Vermahmoudi Y. Parametric study of overall heat transfer coefficient of CuO/water nanofluids in a car radiator. Int J Therm Sci. 2013;66(Supplement C):82–90.

103. Ebrahimi M, Farhadi M, Sedighi K, Akbarzade S. Experimental investigation of force convection heat transfer in a car radiator filled with SiO_2–water nanofluid. IJE Trans B Appl. 2014;27(2):333–40.

104. Hussein AM, Bakar RA, Kadirgama K. Study of forced convection nanofluid heat transfer in the automotive cooling system. Case Stud Therm Eng. 2014;2(Supplement C):50–61.

105. Heris SZ, Shokrgozar M, Poorpharang S, Shanbedi M, Noie SH. Experimental study of heat transfer of a car radiator with CuO/ethylene glycol–water as a coolant. J Dispers Sci Technol. 2014;35(5):677–84.

106. Sarkar J, Tarodiya R. Performance analysis of louvered fin tube automotive radiator using nanofluids as coolants. Int J Nanomanuf. 2013;9(Supplement C):51–65.

107. Devendiran DK, Amirtham VA. A review on preparation, characterization, properties and applications of nanofluids. Renew Sustain Energy Rev. 2016;60(1):21–40.

108. Barzegarian R, Aloueyan A, Yousefi T. Thermal performance augmentation using water based Al_2O_3-gamma nanofluid in a horizontal shell and tube heat exchanger under forced circulation. Int Commun Heat Mass Transf. 2017;86(Supplement C):52–9.

109. Jafari SM, Jabari SS, Dehnad D, Shahidi SA. Heat transfer enhancement in thermal processing of tomato juice by application of nanofluids. Food Bioprocess Technol. 2017;10(2):307–16.

110. Elshazly KM, Sakr RY, Ali RK, Salem MR. Effect of γ-Al_2O_3/water nanofluid on the thermal performance of shell and coil heat exchanger with different coil torsions. Heat Mass Transf. 2017;53(6):1893–903.

111. Hussein AM. Thermal performance and thermal properties of hybrid nanofluid laminar flow in a double pipe heat exchanger. Exp Therm Fluid Sci. 2017;88(Supplement C):37–45.

112. Bhat MW, Jaffri AJ, Vyas G, Kumar A, Dondapati RS. Experimental investigation on flow behavior and heat transfer characteristics of CuO based nanoparticles with water in composite pipe. Int J Mech Eng Technol. 2017;8(7):1500–7.

113. Darzi AAR, Farhadi M, Sedighi K. Heat transfer and flow characteristics of Al_2O_3–water nanofluid in a double tube heat exchanger. Int Commun Heat Mass Transf. 2013;47(Supplement C):105–12.

114. Duangthongsuk W, Wongwises S. An experimental study on the heat transfer performance and pressure drop of TiO_2–water nanofluids flowing under a turbulent flow regime. Int J Heat Mass Transf. 2010;53(1):334–44.

115. Aghayari R, Maddah H, Ashori F, Hakiminejad A, Aghili M. Effect of nanoparticles on heat transfer in mini double-pipe heat exchangers in turbulent flow. Heat Mass Transf Waerme- und Stoffuebertragung. 2014;51(3):301–6.

116. Raei B, Shahraki F, Jamialahmadi M, Peyghambarzadeh SM. Experimental study on the heat transfer and flow properties of γ-Al_2O_3/water nanofluid in a double-tube heat exchanger. J Therm Anal Calorim. 2017;127(3):2561–75.

117. Zamzamian A, Oskouie SN, Doosthoseini A, Joneidi A, Pazouki M. Experimental investigation of forced convective heat transfer coefficient in nanofluids of Al_2O_3/EG and CuO/EG in a double pipe and plate heat exchangers under turbulent flow. Exp Therm Fluid Sci. 2011;35(3):495–502.

118. Ravi Kumar NT, Bhramara P, Sundar LS, Singh MK, Sousa ACM. Heat transfer, friction factor and effectiveness of Fe_3O_4 nanofluid flow in an inner tube of double pipe U-bend heat exchanger with and without longitudinal strip inserts. Exp Therm Fluid Sci. 2017;85(Supplement C):331–43.

119. Hung Y-H, Wang W-P, Hsu Y-C, Teng T-P. Performance evaluation of an air-cooled heat exchange system for hybrid nanofluids. Exp Therm Fluid Sci. 2017;81(Supplement C):43–55.

120. Palanisamy K, Kumar PCM. Heat transfer enhancement and pressure drop analysis of a cone helical coiled tube heat exchanger using MWCNT/water nanofluid. J Appl Fluid Mech. 2017;10(SpecialIssue):7–13.

121. Selvam C, Muhammed Irshad EC, Lal DM, Harish S. Convective heat transfer characteristics of water–ethylene glycol mixture with silver nanoparticles. Exp Therm Fluid Sci. 2016;77(Supplement C):188–96.

122. Peyghambarzadeh SM, Hashemabadi SH, Naraki M, Vermahmoudi Y. Experimental study of overall heat transfer coefficient in the application of dilute nanofluids in the car radiator. Appl Therm Eng. 2013;52(1):8–16.

123. Sharma S. Fabricating an experimental setup to investigate the performance of an automobile car radiator by using aluminum/water nanofluid. J Therm Anal Calorim. 1995. https://doi.org/10.1007/s10973-018-7224-9.

124. Tzeng S-C, Lin C-W, Huang K. Heat transfer enhancement of nanofluids in rotary blade coupling of four-wheel-drive vehicles. Acta Mech. 2005;179(1–2):11–23.

125. Zhang K-J, Wang D, Hou F-J, Jiang W-H, Wang F-R, Li J, et al. Characteristic and experiment study of HDD engine coolants. Chin Intern Combust Engine Eng. 2007;1:017.

126. Ali M, El-Leathy A, Al-Sofyany Z. The effect of nanofluid concentration on the cooling system of vehicles radiator. Adv Mech Eng. 2014;6:962510.

127. M'hamed B, Sidik NAC, Akhbar MFA, Mamat R, Najafi G. Experimental study on thermal performance of MWCNT nanocoolant in Perodua Kelisa 1000 cc radiator system. Int Commun Heat Mass Transf. 2016;76:156–61.

128. Devireddy S, Mekala CSR, Veeredhi VR. Improving the cooling performance of automobile radiator with ethylene glycol water based TiO_2 nanofluids. Int Commun Heat Mass Transf. 2016;78:121–6.

129. Mathivanan E, Gasior D, Liu L, Yee K, Li Y. Experimental investigation of the impact of nanofluids on heat transfer performance of a motorcycle radiator: SAE Technical Paper 2017. Report No.: 0148-7191.

130. Sahoo RR, Ghosh P, Sarkar J. Performance enhancement for wavy fin automotive radiator using optimum pg brine based nanofluids. Heat Transf Asian Res. 2017;46(6):585–97.

131. Vajjha RS, Das DK, Namburu PK. Numerical study of fluid dynamic and heat transfer performance of Al_2O_3 and CuO nanofluids in the flat tubes of a radiator. Int J Heat Fluid Flow. 2010;31(4):613–21.

132. Vajjha RS, Das DK, Ray DR. Development of new correlations for the Nusselt number and the friction factor under turbulent flow of nanofluids in flat tubes. Int J Heat Mass Transf. 2015;80:353–67.

133. Hatami M, Jafaryar M, Zhou J, Jing D. Investigation of engines radiator heat recovery using different shapes of nanoparticles in $H_2O/(CH_2OH)_2$ based nanofluids. Int J Hydrog Energy. 2017;42(16):10891–900.

134. Sahoo RR, Sarkar J. Heat transfer performance characteristics of hybrid nanofluids as coolant in louvered fin automotive radiator. Heat Mass Transf. 2017;53(6):1923–31.

135. Leong K, Saidur R, Kazi S, Mamun A. Performance investigation of an automotive car radiator operated with nanofluid-based coolants (nanofluid as a coolant in a radiator). Appl Therm Eng. 2010;30(17):2685–92.

136. Togun H, Kazi SN, Badarudin A. Turbulent heat transfer to separation nanofluid flow in annular concentric pipe. Int J Therm Sci. 2017;117(Supplement C):14–25.

137. Khan MS, Dil T. Heat transfer enhancement of automobile radiator using H_2O–CuO nanofluid. AIP Adv. 2017;7(4):045018.

138. Ahmad UK, Hasreen M, Yahaya NA, Rosnadiah B. Comparative study of heat transfer and friction factor characteristics of nanofluids in rectangular channel. Procedia Eng. 2017;170(Supplement C):541–6.

139. Hussein AM, Dawood HK, Bakara RA, Kadirgamaa K. Numerical study on turbulent forced convective heat transfer using nanofluids TiO_2 in an automotive cooling system. Case Stud Therm Eng. 2017;9(Supplement C):72–8.

140. Saripella S, Yu W, Routbort J, France D. Effects of nanofluid coolant in a class 8 truck engine: SAE Technical Paper2007. Report No.: 0148-7191.

141. Fsadni AM, Whitty JPM, Stables MA, Adeniyi AA. Numerical study on turbulent heat transfer and pressure drop characteristics of a helically coiled hybrid rectangular–circular tube heat exchanger with Al_2O_3–water nanofluids. Appl Therm Eng. 2017;114(Supplement C):466–83.

142. Bellos E, Tzivanidis C. A review of concentrating solar thermal collectors with and without nanofluids. J Therm Anal Calorim. 2018. https://doi.org/10.1007/s10973-018-7183-1.

143. Boyaghchi FA, Chavoshi M. Monthly assessments of exergetic, economic and environmental criteria and optimization of a solar micro-CCHP based on DORC. Sol Energy. 2018;166:351–70.

144. Hu Y, He Y, Zhang Z, Wen D. Effect of Al_2O_3 nanoparticle dispersion on the specific heat capacity of a eutectic binary nitrate salt for solar power applications. Energy Convers Manag. 2017;142:366–73.

145. Jin J, Jing D. A novel liquid optical filter based on magnetic electrolyte nanofluids for hybrid photovoltaic/thermal solar collector application. Sol Energy. 2017;155:51–61.

146. Koca HD, Doganay S, Turgut A. Thermal characteristics and performance of Ag–water nanofluid: application to natural circulation loops. Energy Convers Manag. 2017;135:9–20.

147. Tahat MS, Benim AC, editors. Experimental Analysis on thermophysical properties of Al_2O_3/CuO hybrid nano fluid with its effects on flat plate solar collector. Defect and diffusion forum; 2017: Trans Tech Publications.

148. Manikandan S, Rajan K. Sand–propylene glycol–water nanofluids for improved solar energy collection. Energy. 2016;113:917–29.

149. Saidur R, Meng TC, Said Z, Hasanuzzaman M, Kamyar A. Evaluation of the effect of nanofluid-based absorbers on direct solar collector. Int J Heat Mass Transf. 2012;55(21–22):5899–907.

150. Bellos E, Tzivanidis C. Thermal efficiency enhancement of nanofluid-based parabolic trough collectors. Journal of Thermal Analysis and Calorimetry.

151. Bellos E, Tzivanidis C, Papadopoulos A. Enhancing the performance of a linear Fresnel reflector using nanofluids and internal finned absorber. J Therm Anal Calorim. 2018. https://doi.org/10.1007/s10973-018-6989-1.

152. Rashidi S, Eskandarian M, Mahian O, Poncet S. Combination of nanofluid and inserts for heat transfer enhancement. J Therm Anal Calorim. 2018. https://doi.org/10.1007/s10973-018-7070-9.

153. Sidik NAC, Samion S, Ghaderian J, Yazid MNAWM. Recent progress on the application of nanofluids in minimum quantity lubrication machining: a review. Int J Heat Mass Transf. 2017;108:79–89.

154. Jang SP, Choi SUS. Cooling performance of a microchannel heat sink with nanofluids. Appl Therm Eng. 2006;26(17):2457–63.

155. Chabi A, Zarrinabadi S, Peyghambarzadeh S, Hashemabadi S, Salimi M. Local convective heat transfer coefficient and friction factor of CuO/water nanofluid in a microchannel heat sink. Heat Mass Transf. 2017;53(2):661–71.

156. Sun B, Liu H. Flow and heat transfer characteristics of nanofluids in a liquid-cooled CPU heat radiator. Appl Therm Eng. 2017;115:435–43.

157. Bayomy A, Saghir M. Experimental study of using γ-Al_2O_3–water nanofluid flow through aluminum foam heat sink: comparison with numerical approach. Int J Heat Mass Transf. 2017;107:181–203.

158. Arjun K, Rakesh K. Heat transfer enhancement using alumina nanofluid in circular micro channel. J Eng Sci Technol. 2017;12(1):265–79.

159. Irwansyah R, Cierpka C, Kähler CJ, editors. On the reliable estimation of heat transfer coefficients for nanofluids in a microchannel., Journal of Physics: Conference SeriesBristol: IOP Publishing; 2016.

160. Toghraie D, Abdollah MMD, Pourfattah F, Akbari OA, Ruhani B. Numerical investigation of flow and heat transfer characteristics in smooth, sinusoidal and zigzag-shaped microchannel with and without nanofluid. J Therm Anal Calorim. 2018;131(2):1757–66.

161. Wu JM, Zhao J. A review of nanofluid heat transfer and critical heat flux enhancement—research gap to engineering application. Prog Nucl Energy. 2013;66(Supplement C):13–24.

162. Zangeneh A, Vatani A, Fakhroeian Z, Peyghambarzadeh S. Experimental study of forced convection and subcooled flow boiling heat transfer in a vertical annulus using different novel functionalized ZnO nanoparticles. Appl Therm Eng. 2016;109:789–802.

163. Peng H, Ding G, Jiang W, Hu H, Gao Y. Heat transfer characteristics of refrigerant-based nanofluid flow boiling inside a horizontal smooth tube. Int J Refrig. 2009;32(6):1259–70.

164. Ahn HS, Kim H, Jo H, Kang S, Chang W, Kim MH. Experimental study of critical heat flux enhancement during forced convective flow boiling of nanofluid on a short heated surface. Int J Multiph Flow. 2010;36(5):375–84.

165. Vafaei S, Wen D. Critical heat flux (CHF) of subcooled flow boiling of alumina nanofluids in a horizontal microchannel. J Heat Transf. 2010;132(10):102404–7.

166. Hashemi M, Noie SH. Study of flow boiling heat transfer characteristics of critical heat flux using carbon nanotubes and water nanofluid. J Therm Anal Calorim. 2017;130(3):2199–209.

167. Yang X-F, Liu Z-H. Flow boiling heat transfer in the evaporator of a loop thermosyphon operating with CuO based aqueous nanofluid. Int J Heat Mass Transf. 2012;55(25):7375–84.

168. Wu S, Zhu D, Li X, Li H, Lei J. Thermal energy storage behavior of Al_2O_3–H_2O nanofluids. Thermochim Acta. 2009;483(1):73–7.

169. Wu S, Zhu D, Zhang X, Huang J. Preparation and melting/freezing characteristics of Cu/paraffin nanofluid as phase-change material (PCM). Energy Fuels. 2010;24(3):1894–8.

170. Parsazadeh M, Duan X. Numerical and statistical study on melting of nanoparticle enhanced phase change material in a shell-and-tube thermal energy storage system. Appl Therm Eng. 2017;111:950–60.

171. Sebti SS, Khalilarya SH, Mirzaee I, Hosseinizadeh SF, Kashani S, Abdollahzadeh M. A numerical investigation of solidification in horizontal concentric annuli filled with nano-enhanced phase change material (NEPCM). World Appl Sci J. 2011;13(1):9–15.

172. Tasnim SH, Hossain R, Mahmud S, Dutta A. Convection effect on the melting process of nano-PCM inside porous enclosure. Int J Heat Mass Transf. 2015;85(Supplement C):206–20.